

# An Operator Product Expansion for Polygonal null Wilson Loops

Luis F. Alday<sup>1</sup>, Davide Gaiotto<sup>1</sup>, Juan Maldacena<sup>1</sup>, Amit Sever<sup>2</sup>, Pedro Vieira<sup>2</sup>

<sup>1</sup>*School of Natural Sciences, Institute for Advanced Study, Princeton, NJ 08540, USA*

<sup>2</sup>*Perimeter Institute for Theoretical Physics, Waterloo, Ontario N2J 2W9, Canada*

We consider polygonal Wilson loops with null edges in conformal gauge theories. We derive an OPE-like expansion when several successive lines of the polygon are becoming aligned. The limit corresponds to a collinear, or multicollinear, limit and we explain the systematics of all the subleading corrections, going beyond the leading terms that were previously considered. These subleading corrections are governed by excitations of high spin operators, or excitations of a flux tube that goes between two Wilson lines. The discussion is valid for any conformal gauge theory, for any coupling and in any dimension.

For  $\mathcal{N} = 4$  super Yang Mills we check this expansion at strong coupling and at two loops at weak coupling. We also make predictions for the remainder function at higher loops.

In the process, we also derived a new version for the TBA integral equations that determine the strong coupling answer and present the area as the associated Yang-Yang functional.

## Contents

1. Introduction	1
2. Symmetries	4
2.1. The symmetries preserved by null lines and the square Wilson loop	5
3. The collinear operator product expansion	8
3.1. A three parameter family of polygons	8
3.2. States propagating in the expansion	10
3.3. Taking care of violations of conformal symmetry: the remainder function	14
3.4. Taking care of violations of conformal symmetry without using the $U(1)$ or one loop answer	16
4. Detailed checks for the hexagon	19
4.1. Expansion of the hexagon at strong coupling	19
4.2. Expansion of the hexagon at weak coupling	20
5. Higher order predictions	23
6. Conclusions	23
7. Acknowledgments	24
Appendix A. Describing the family of polygons in terms of momentum twistors	24
Appendix B. The hamiltonian picture and its analytic continuation	25
B.1. Analytic continuation at strong coupling	27
Appendix C. Remarks on the dispersion relation	30
C.1. Massive Goldstone particles	31
Appendix D. On the expansion for Wilson loops in the $U(1)$ theory	32
Appendix E. The modified TBA and Yang-Yang functional for $AdS_3$ null polygons	33
E.1. Evaluating the OPE for general configurations in $AdS_3$	38
Appendix F. The modified TBA and Yang-Yang functional for $AdS_5$ null polygons	39
F.1. Explicit details for the hexagon	40
F.2. Easy pieces of the hexagon	45
F.3. Expanding the hexagon at strong coupling	45

## 1. Introduction

The Operator Product Expansion (OPE) is a powerful tool for studying correlation functions in conformal field theories. The expansion is controlled by the spectrum of local operators of the theory. In particular, their dimensions control the powers of the expansion parameter in the OPE, which is simply the separation between operators. In some cases, such as two dimensional minimal models, it is possible to completely fix the correlation functions by demanding this property in all possible channels [1].

In this paper we derive a similar OPE-like expansion for polygonal Wilson loops with light-like edges. Our main motivation is the relation between Wilson loops and amplitudes in  $\mathcal{N} = 4$  super Yang Mills [2,3,4,5,6]. Furthermore, similar looking Wilson loops appear

in a variety of high energy processes in gauge theories. The OPE expansion is valid for any conformal field theory and in any dimension where we can define null polygonal Wilson loops. It is valid whenever the Wilson lines produce a conserved flux that cannot be screened. It is useful to consider first large  $N$  gauge theories in the planar approximation. We will later make some remarks beyond the planar limit. One challenging aspect of the problem is that Wilson loops with light-like edges are eminently Lorentzian observables without an obvious Euclidean counterpart.

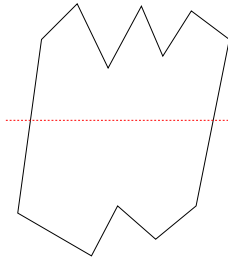


**Fig. 1:** We consider a general Wilson loop with null edges. We select two of its edges and we place an imaginary cut along a line connecting these two selected edges. We then expand the answer in terms of states propagating across this cut.

Our OPE expansion is performed as follows, see fig. 1. First we select two non-consecutive lines of the polygonal Wilson loop. We then cut the Wilson loop into a top part and a bottom part and we expand it in terms of the states propagating through the cut. The states that propagate through the cut correspond to excitations of a flux tube that ends on two light-like lines. Fortunately these states have been considered before. In fact, they are excitations around the infinite spin limit of high spin operators. In theories with gravity/string duals they are excitations around the spinning string (GKP) considered in [7]. In  $\mathcal{N} = 4$  super Yang Mills one can compute these dimensions for all values of the coupling [8,9]. Thus, we find that the Wilson loop has an OPE-like expansion in terms of operators, or states, which are excitations of the infinite spin limit of the GKP string. These states can also be viewed as created by local operator insertions along a null Wilson line.

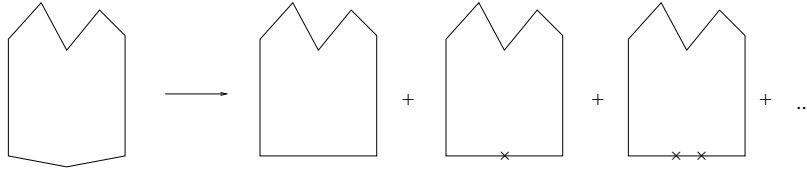


**Fig. 2:** The collinear expansion including subleading terms. The first term is the usual statement that in the collinear limit we recover the Wilson loop with one less line. The second term corresponds to the insertion of one operator along the contour, the second to two operators, etc.

The simplest example of this OPE is a collinear limit, where two consecutive lines become parallel, see fig. 2. This collinear limit was considered previously and its leading divergent and constant terms were understood [10]. These leading terms are determined by the special conformal symmetry anomalous Ward identities [11]<sup>1</sup>. We are now saying that we can continue the expansion into the subleading terms. The existence of this expansion places constraints on the possible form of the Wilson loop correlator. In fact, it constrains the so called remainder function [12,13,14,6] which contains the conformal invariant information on the Wilson loop correlator. We will demonstrate this explicitly below for the case of the six sided Wilson loop in  $\mathcal{N} = 4$  super Yang Mills. In fact we will verify that the strong coupling answer and the two loop weak coupling answer have the form required by the OPE. We will also make a prediction, using [9], for the expansion for all values of the coupling. At strong coupling we can go further and check that the expansion has the required form for general polygons.

It is quite likely, that the existence of this expansion in all possible channels, together with integrability would completely constrain the correlator. This would simply be the extension of the Bootstrap procedure for correlation functions [1] to Wilson loop correlators.

Our paper is organized as follows. In section 2 we discuss the symmetries of the problem. We will use them heavily for deriving the existence of the expansion. The key idea is to identify a “Hamiltonian” which organizes the expansion. In section 3 we explain the form of the OPE expansion for Wilson loops. In section 4 we discuss the form of the expansion for the case of the hexagonal Wilson loop at strong and weak coupling. Finally in section 5 we briefly discuss higher order predictions.

---

<sup>1</sup> Though this statement is believed to be true, to our knowledge it hasn’t been proven. We will see that it follows from our discussion at the end of section 3.

The paper contains several appendices. In appendix A we describe our setup in terms of momentum twistors. In appendix B we present further arguments for the identification of the states we encounter in the expansion and excitations around the flux tube connecting two null Wilson lines. In appendix C we discuss the dispersion relation of the eigenvalues of the “Hamiltonian”. In appendix D we present some details on the one loop computation of some “form factors”.

Finally, in appendices E and F we give a new form for the integral equations described in [15,16]. In the new form, the equations involve only physical cross ratios. Furthermore, the expression for the area is given by the Yang-Yang functional of the associated TBA-like integral equations. This form is particularly useful for analyzing our limit. It is very likely that it will also be useful for further studies on integrability and Wilson loops/amplitudes. Thus these appendices can be read on their own.

## 2. Symmetries

The expansion we are studying is governed by the symmetries preserved by two null lines and also by the symmetries preserved by the square Wilson loop, i.e. a Wilson loop with four null sides.

To justify the need to understand the symmetries, let us recall first how symmetries constrain and determine the ordinary OPE for correlation functions. In that case the main symmetry in question is dilatations. If we have a correlator  $\langle O(1)O(2)\dots O(n)\rangle$ . Then we can set  $O(1)$  at the origin and consider the limit where  $O(2)$  approaches it. This operation corresponds to a dilatation applied to operators  $O(1)$  and  $O(2)$ , but not to the rest of the operators. This becomes more clear if we map this to the (Euclidean) cylinder. Then  $O(1)$  is at  $\tau_1 = -\infty$  and  $O(2)$  is at some value of  $\tau_2$  and the rest are at fixed values of  $\tau_i$ . Here  $\tau$  is the (Euclidean) time coordinate on the cylinder. We also demand that  $\tau_2 < \min\{\tau_i\}$ . The OPE expansion follows by cutting the cylinder between  $\tau_2$  and  $\min\{\tau_i\}$  and inserting a complete basis of eigenstates of the dilatation operator. The fact that the OPE is convergent follows from the asymptotic growth of states<sup>2</sup>.

---

<sup>2</sup> For a  $d$  dimensional CFT we have  $\log N(\Delta) \sim (\text{constant})\Delta^{\frac{d-1}{d}} \ll \Delta$  as  $\Delta \rightarrow \infty$ .

2.1. *The symmetries preserved by null lines and the square Wilson loop*

Let us start with two generic non-intersecting null lines and consider the symmetries that leave these two null lines invariant. Working in  $R^{1,3}$ , by conformal transformations we send a null line to null infinity and the other to a null line extended along  $x^-$  and passing through the origin. We can do this so that both null lines are in an  $R^{1,1}$  subspace, with one of the lines at null infinity. The symmetries that leave this configuration invariant include dilatations  $D$ , boosts in  $x^\pm$ ,  $M^{+-}$ , and a rotation in the two transverse directions  $M^{12}$ . In addition we have translations  $P_-$  along  $x^-$  and special conformal transformations  $K^-$ . The symmetries  $P_-$ ,  $K^-$  and  $D + M^{+-}$  form an  $SL(2, R)$  subgroup, which commutes with the two remaining abelian symmetries:  $D - M^{+-}$  and  $M^{12}$ . Note that these two remaining symmetries leave individual points on the lines invariant, while the  $SL(2, R)$  symmetry maps points on a given line to other points on the same line, but does not leave them invariant in a pointwise fashion.

For this counting of symmetries it is important that we have the line at null infinity. If we only had the line that goes through the origin we would have more symmetry generators such as  $K^i$ ,  $K^+$ , and boosts  $M^{+i} \sim x^+ \partial_i - x^i \partial_{x^+}$ , where  $i$  is a transverse index. However, these transformations do not leave the line at infinity invariant. This can be checked by using an inversion to map the line at infinity to the origin. For example, this turns  $K^i$  into  $P^i$  which indeed does not leave the line at the origin fixed. These symmetries preserve one of the null lines but move the other one. So they are not true symmetries of the two line system. Nevertheless we will see that they have some interesting consequences.

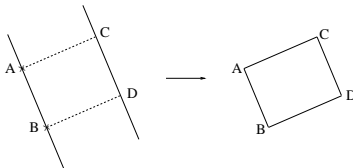


**Fig. 3:** We start with two null lines, denoted by the solid lines. By picking a point  $A$  on the first line, we determine a unique point  $C$  on the second line which is light-like separated from  $A$ . Similarly for  $B$ . In this way we construct a square. In the figure we projected onto two spatial directions and suppressed the time direction.

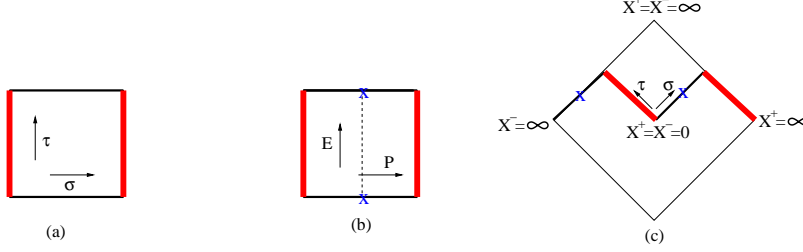


**Fig. 4:** (a) The square Wilson loop projected onto two spatial directions. We suppressed the time direction. The “Hamiltonian” symmetry  $\partial_\tau$  moves points along the arrow direction. It leaves points on the thin black lines fixed, but moves points along the thick red lines. The “momentum” symmetry  $\partial_\sigma$  is also indicated. (b) We inserted an operator on the bottom line. We can integrate the operator along the bottom edge in such a way that it has a definite momentum with respect to the  $\partial_\sigma$  symmetry. If it creates a single particle state, then it will also have a definite energy. (c) We have mapped the square to an  $R^{1,1}$  subspace by a conformal transformation that sent a cusp to spatial infinity. Two of the null lines are at null infinity. One of the cusps is at the origin. Operators inserted along the top and bottom lines in (b) correspond to operator insertions which are spacelike separated, and indicated by a cross. The “Hamiltonian” and “momentum” correspond to the generators  $D \pm M^{+-}$ .

Once we have understood the symmetries of two lines, we now want to understand the symmetries of the square. To define the square we need to pick two points along one of the null lines where the vertices of the square will be sitting. Once we pick a point along a null line to be a vertex of the square, the corresponding point along the other null line is automatically fixed, since it is the point on the other null line that is null separated with respect to the point chosen on the first line, see fig. 3. Thus, picking a square, now corresponds to picking two points along a null line. This breaks the  $SL(2, R)$  symmetry group to a single generator. We are going to view this remaining generator of  $SL(2, R)$  as a “Hamiltonian”. This Hamiltonian moves points on both segments of the original null lines towards the same side of the square. In fact, we will see that, because the new sides of the square are spacelike separated, this “Hamiltonian” is a Euclidean Hamiltonian such that the evolution operator looks like  $e^{-\tau E}$ , as opposed to  $e^{-i\tau E}$ , where  $E$  are the real energy eigenvalues. The second non-compact symmetry moves points along the bottom and top lines of the square, see fig. 4(a). We can view this as a “momentum” generator. In fact, the “Hamiltonian” has a continuous spectrum due to the existence of this second non-compact symmetry.

In summary, the square has three commuting symmetries. Two noncompact symmetries and one transverse rotation symmetry. In (2,2) signature the transverse symmetry becomes a boost and is also non-compact.

The symmetries of the square can also be understood directly as follows. By a conformal transformation we can map three of the points to the boundary of Minkowski space. One of the points is mapped to spatial infinity, and the other two are mapped to some points on null infinity. The fourth point can be set at the origin. In that case we just have a null cusp with lines along  $x^+x^- = 0$ ,  $x^\pm > 0$ . See fig. 4(c). Let us understand the symmetries that leave this invariant. We clearly have three commuting symmetries: dilatations, boosts in the  $x^\pm$  plane and the rotation in the transverse plane. In fact, these are all the symmetries of this Wilson loop. It is fairly clear that there are no further Poincare symmetries of  $R^{1,3}$  that leave it invariant. There are no special conformal symmetries that leave it invariant because any special conformal symmetry moves the point at spatial infinity, which is one of the vertices of the polygon.

Single Line	$D - M^{+-}$	$M^{12}$	$D + M^{+-}$	$K^-$	$P_-$	$M^{+i}$	$K^+$	$K^i$
Two Lines	$D - M^{+-}$	$M^{12}$	$D + M^{+-}$	$K^-$	$P_-$			
Square	$D - M^{+-}$	$M^{12}$	$D + M^{+-}$					
Name	$P, \partial_\sigma$	$\tilde{S}, \partial_\phi$	$E, \partial_\tau$					

Table 1: Symmetries preserved by one and two lines and the square.

In the last line we introduced some notation for each of the three symmetries.

It is also useful to understand how the “Hamiltonian” acts on the “bottom” side of the square, see fig. 4. It leaves it invariant on a point by point basis and it rescales the transverse directions. More precisely, if we say that this bottom side is along  $x^+$ , then it rescales  $x^- \rightarrow \lambda^2 x^-$  and  $y_\perp \rightarrow \lambda y_\perp$ , see fig. 4(c). This action is sometimes called “twist” operator. More concretely, we will find that in our expansion procedure we will need to consider operators inserted along this “bottom” null line, see fig. 4(b) (c). Similar operators arise also in the study of high energy processes in QCD, for a review see [17]. Such an operator is characterized by a “momentum” along the direction of the line. This is the same “momentum” generator that we mentioned above. In the QCD literature on operators involving null Wilson lines this generator is called the spin of the state (e.g. in



[17]). It turns out that if we insert a local operator along the null Wilson line, this operator will not be an eigenstate of the twist operator (or our “Hamiltonian”). However, single particle states with definite “momentum” are indeed eigenstates.

The states that are contributing to the OPE are the states created by inserting local operators along the bottom side of the Wilson loop and propagating all the way to the top, see fig. 4(b). These states have a continuous spectrum, due to the existence of a second non-compact symmetry. This is in contrast to the ordinary operator product expansion where the spectrum of dimensions is discrete. However, due to the momentum symmetry we can certainly isolate the contributions from “single particle” states propagating along the square.

### 3. The collinear operator product expansion

In this section we state more precisely how to perform the OPE expansion. In the case of ordinary correlation functions the expansion can be organized in terms of the dimensions and the spins of the intermediate operators. As we mentioned above, the operators that appear in our expansion are characterized by their dimension (or energy) and also by another continuous label which we will call the momentum. There is a third discrete label which is the spin in the transverse dimension. In order to isolate the various quantum numbers it is convenient to introduce the following three parameter family of polygons.

#### 3.1. A three parameter family of polygons

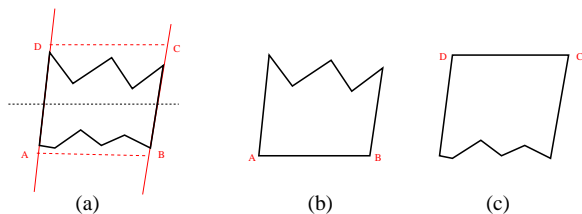


**Fig. 5:** (a) Given a general polygon we select two segments. We prolong them and choose two points on one of these segments  $A$  and  $D$ . These determine points  $B$  and  $C$  on the other line. We use them to form a reference square  $ABCD$ . We now cut the polygon into a top part and a bottom part. We apply a combination of symmetries of the square to the bottom part. In the limit  $\tau \rightarrow \infty$  the bottom part is flattened out into the straight edge of the reference square. In that limit we get the polygon in (b) which we will call the “top” polygon. Alternatively, we could have applied the symmetry to the top half of the polygon in (a). In the limit we would get the polygon in (c) which we call the “bottom” polygon.

We would now like to introduce an interesting family of polygons. The family is specified as follows. Let us assume that all the points on the polygon are spacelike separated, except for the obvious null separations that define the polygon. We first pick two non-consecutive null sides of the polygon, and extend them to two null lines. We then pick two points along the null line which lie outside the segment that belongs to the polygon on that null line. These two points, together with the two null lines define a certain reference square. The symmetries of the square involve the three symmetries we discussed above, see fig. 5. Let us say the two lines we picked are lines  $i$  and  $j$ . This splits the polygon into a “top” part and a “bottom” part. We now consider a symmetry generator  $M$  which leaves the reference square invariant. We leave the “top” invariant and act with  $M$  on the bottom part of the original polygon. The cross-ratios for this family of polygons can be described more explicitly in terms of momentum twistors, see appendix A.

The family has three parameters  $M = e^{\tau\partial_\tau + \sigma\partial_\sigma + \phi\partial_\phi} = e^{-\tau E + i\sigma P + i\phi S}$ . The three parameters  $\tau, \sigma, \phi$  are conjugate to the three symmetries of the problem. The  $\tau$  parameter is the one that is coupling to the symmetry that was included in the  $SL(2, R)$  symmetry of the two null lines. When we send  $\tau \rightarrow \infty$  we are mapping the whole set of points between lines  $j$  and  $i$  to one of the sides of the square. We can view this as a multicollinear limit, see fig. 5. The collinear limit corresponds to the special case where we have only two segments between segments  $j$  and  $i$  and we take the  $\tau \rightarrow \infty$  limit, see fig. 2.

The idea is that we can expand the whole Wilson loop in terms of eigenstates of these three operators. These eigenstates corresponds to excitations of the flux tube (or string) that goes between the two selected null lines. Thus, we are cutting the Wilson loop. The bottom and top parts of the loop correspond to two particular superpositions of states. Introducing the family of polygons is helpful for isolating the contributions from different eigenstates. To perform this expansion we are simply using the conformal symmetry of the problem. Thus, the expansion makes sense for null polygons in any dimension where we can define Wilson loops and for any value of the coupling.

Again, given a polygon we fix a reference square and introduce a family of polygons parametrized by  $\tau, \sigma$  and  $\phi$ . These coordinates are associated to the unbroken symmetries of the square. The original polygon may be associated to the point  $\tau = \sigma = \phi = 0$  but that is of course not important, we then expand at large  $\tau$  and resum to get  $\tau = 0$  if we want. The choice of reference square is the analog of the choice of point for an operator product expansion and the points  $\tau, \sigma$  and  $\phi$  are the analog of the coordinates with respect to that chosen point.

So far we are describing the kinematics of the expansion we want to define. In order to flesh this out a bit more we will need to understand some more aspects of the dynamics so that we have a clearer picture of the states that appear in the expansion.

### 3.2. States propagating in the expansion

What is interesting about this family of polygons is that we can view the symmetry conjugate to  $\tau$  as a Hamiltonian. In that case we expect that the result has an expression of the form

$$\langle W \rangle = \int dn e^{-\tau E_n} C_n, \quad C_n = C_n^{\text{top}} C_n^{\text{bottom}} \quad (3.1)$$

where  $n$  is some set of labels for the different “energy” eigenstates. We have also emphasized the fact that the coefficients  $C_n$  factorize into two contributions which are the overlap of the intermediate state with the top or bottom polygon. In order to make a precise statement we will have to take into account that UV divergencies of the Wilson loop break these symmetries. Fortunately, this breaking is well understood and we will be able to take care of those effects in a simple fashion. So, let us treat it as an exact symmetry for the time being.

Now, let us explain better what kind of states we expect in (3.1). In the case of the ordinary OPE of local operators we can surround the two operators we are considering by a three sphere. We can then view the states appearing in the OPE as energy eigenstates of the theory on the sphere. To be more precise, we could consider the conformal field theory in  $R \times S^3$  and find the energy eigenstates.

In our case, the procedure is very similar, we could consider a constant  $\tau$  surface. We see that the surface is pierced by two null Wilson lines, see fig. 1. The Wilson lines that pierce the surface create a color electric flux tube. The states can be understood as excitations of this flux tube. In other words, the flux with no excitations gives a flux vacuum. We need to understand the excitations of the field theory around this vacuum.

More explicitly the states propagating can be understood as follows. We start with the Yang Mills theory on  $R \times S^3$ . We now add two null Wilson lines moving along a great circle of the  $S^3$ , see fig. 6(a). If  $\varphi$  is the coordinate of that circle, then the lines are along  $t = \varphi$  and  $t = \varphi + \pi$  where  $t$  is the time coordinate. The generator  $\Delta - S = i\partial_t + i\partial_\varphi$  is a symmetry of the configuration and we will call it the “Energy”. It is also called the “twist”. One line corresponds to a quark and the other to an anti-quark. These lines create a color electric field. The configuration is invariant under the “momentum” symmetry, see

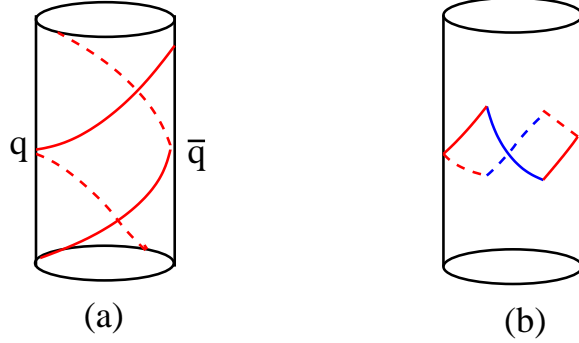


**Fig. 6:** (a) Field theory on  $R \times S^3$  in the presence of two null Wilson lines. Dotted lines are in the back of the cylinder. Of course the circle of the cylinder is really an  $S^3$ . (b) Double analytic continuation sends the initial and final states of (a) to two null lines, the two blue null lines. Different states will contain different insertions along these two blue null lines.

[18], generated by  $P = -i\partial_\sigma$ . This is not an obvious geometric symmetry of  $R \times S^3$ , it is a combination involving conformal Killing vectors. The flux is extended along the  $\sigma$  direction and has a constant energy density along  $\sigma$ . Thus its energy diverges. The energy density is simply the cusp anomalous dimension [18]. The flux emanates from a point in the extra  $S^2 \subset S^3$  and the transverse  $SO(2)$  symmetry is the rotation that leaves this point invariant. In appendix B we show how to choose a conformal frame where both the  $\tau$  and  $\sigma$  translations are manifest. This is the ground state of the configurations we consider. We can then add excitations which propagate on top of this configuration. In the planar theory these are excitations of the color electric flux and the indices of the particles we create are contracted with the indices of the background flux. This is a Lorentzian picture for the states appearing in the OPE. See appendix B for further discussion.

We can perform an analytic continuation of the configuration with two Wilson lines on  $R \times S^3$  to a configuration with four Wilson lines describing the square Wilson loop, see fig. 6(b). Upon this transformation the Energy generator becomes a generator which acts in a Euclidean fashion. It becomes the  $\partial_\tau$  generator we mentioned before for the square. The two lines of the Lorentzian picture become two opposite lines of the square. The excitations are produced by adding operators on the other two lines of the square, see fig. 6(b).

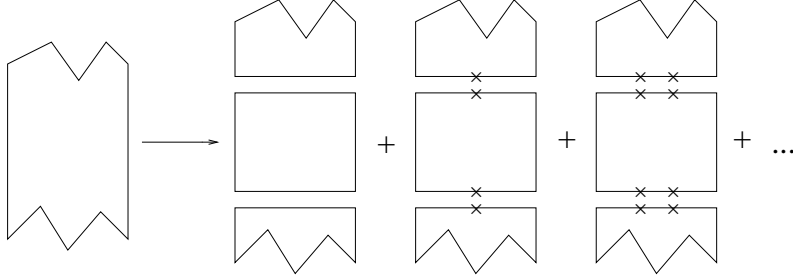


**Fig. 7:** Expansion of a Wilson loop in terms of states propagating on the square. The first term corresponds to the expectation values of the top and bottom Wilson loops. We can define the expectation value of the square as being one. The second term corresponds to the exchange of a single particle. The top and bottom Wilson loops give rise to the factors  $C^{\text{top}}$  and  $C^{\text{bottom}}$  in the OPE expansion. The third term contains two particle states, and possible bound states, etc.

These states form representations under the two other commuting symmetries. One of them,  $\partial_\sigma$ , is a non-compact symmetry. Thus, we expect a continuous spectrum of excitations. We can thus separate states according to their “momentum” in the  $\sigma$  direction. In addition, we have some angular momentum number  $m$  under the transverse rotation. Thus a more refined statement has the form

$$\langle W \rangle = \int dn e^{-\tau E_n + ip_n \sigma + im_n \phi} C_n \quad (3.2)$$

Now that we have defined this family we can simply take the large  $\tau$  limit. This would select the lowest lying states from (3.2). But the expansion makes sense for any  $\tau$  and we conjecture that it converges for all values of  $\tau$  such that all points in the polygon remain spacelike separated for all  $\sigma$  and  $\phi$  for that fixed  $\tau$ .

The first subleading correction comes from a single excitation that is moving on the background of the square Wilson loop. This corresponds to the lowest lying excitation of the color electric flux we discussed above. In other words, taking the leading order limit corresponds to replacing the whole bottom of the Wilson loop by the single line of the square, fig. 5(b). Taking into account the fact that the line is not really straight corresponds to insertions of  $F_{+i}$  along that line, where  $+$  is the direction along the line. This is the case, because deformations of a Wilson loop can be understood in terms of insertions of such operators along the original loop. Thus, the simplest deformation corresponds to a single insertion of the field strength  $F_{+i}$  along the loop. By an insertion along the loop, what we really mean is that we have an expression of the form

$$\text{Tr}[P e^{\oint_x^x A} F_{+i}(x)] \quad (3.3)$$

where  $F$  is inside the trace and inserted along the contour at point  $x$ .  $Pe^{\oint_x^x A}$  denotes the integral of the connection along the loop starting at  $x$ , going around the loop and ending again at  $x$ .

Note that  $F$  is inserted along a null line. We can now consider the generator  $\Delta - S = D - M^{+-}$  which leaves points on this line invariant. This is the so called “twist” generator. In fact, operators which correspond to Wilson lines along a null direction with operators inserted on them were analyzed quite extensively in gauge theories, including QCD, because they govern many interesting high energy processes, going back to the classic analysis of deep inelastic scattering. See [17] for a review.

Thus, one of the interesting points is that the operators that appear are fairly well understood and have been studied in the past. Note that the operator (3.3) breaks the  $\sigma$  translation symmetry, since  $\partial_\sigma$  moves points along the null line where  $F_{+i}$  is inserted. Thus, we can consider superpositions with definite momentum  $p$  along the  $\sigma$  direction. In addition, it has charge  $\pm 1$  under the transverse  $SO(2)$  symmetry. There is a unique state with momentum  $p$  and thus this state is automatically an eigenstate of the Hamiltonian  $\partial_\tau$ , with energy  $\epsilon(p)$ . We can think of  $\epsilon(p)$  as the single particle dispersion relation. Our discussion so far, has been valid for any conformal planar gauge theory. In the particular case of  $\mathcal{N} = 4$  super Yang mills the function  $\epsilon(p, \lambda)$  has been computed exactly in [9]. The square has a symmetry under the exchange of  $\tau$  and  $\sigma$ . This amounts to a “Wick” rotation which exchanges the spatial and time direction. This implies certain constraints on the dispersion relation. More can be found in appendix C.

For general non-planar conformal theories this discussion continues to be valid as long as the flux is conserved. For example, in non planar  $\mathcal{N} = 4$  super Yang Mills the discussion continues to be valid if we consider Wilson lines in the fundamental. The flux vacuum is well defined, and so are its excitations. If we consider Wilson lines in the adjoint, then the flux can be screened and the discussion will need some modifications.

In summary, the leading order expression in the large  $\tau$  limit is given by<sup>3</sup>

$$\log\langle W \rangle = \log\langle W \rangle^{\text{top}} + \log\langle W \rangle^{\text{bottom}} + \sum_{\pm} \int dp C_{\pm}(p, \lambda) e^{\pm i\phi} e^{ip\sigma} e^{-\epsilon(p, \lambda)\tau} + \dots \quad (3.4)$$

where  $C_{\pm}(p, \lambda)$  are some unknown functions, analogous to OPE coefficients. And  $\log\langle W \rangle^{\text{top, bottom}}$  are the expectation values of the top and bottom Wilson loops, see fig. 5

---

<sup>3</sup> Taking the logarithm reorganizes the expansion in the usual fashion.

(b)(c). The function  $\epsilon(p, \lambda)$  is the exact dimension (or twist) for a single insertion of  $F_{+i}$  along a null line. In fact,  $C_{\pm} = C_{\pm}^{\text{top}} \times C_{\pm}^{\text{bottom}}$  where  $C_{\pm}^{\text{top}}$  and  $C_{\pm}^{\text{bottom}}$  correspond to the expectation values of the Wilson loop contours in fig. 7 with an  $F_{+i}$  insertion on the top or bottom line<sup>4</sup>. In other words, as usual,  $C_{\pm}^{\text{top}}$  is the overlap between the intermediate state that is propagating and the state created by top part of the Wilson loop while  $C_{\pm}^{\text{bottom}}$  is the overlap with the bottom Wilson loop.

### 3.3. Taking care of violations of conformal symmetry: the remainder function

So far we have ignored the UV divergencies of the Wilson loop and we have treated the symmetries as if they were unbroken. Since the breaking of the symmetries is a well understood phenomenon [11], it is clear that we should be able to take this breaking into account. In other words, there is an anomalous ward identity which tell us how the Wilson loop changes when we apply a special conformal transformation. Thus, we could go through the above argument adding the corresponding terms due to the anomalous ward identity.

We will follow a slightly different route which we found more convenient. This is based on the observation that the anomalous ward identity is also obeyed by the same Wilson loop correlator but in a free  $U(1)$  theory. More precisely, we simply need to take the free  $U(1)$  result and replace the cusp anomalous dimension of the  $U(1)$  theory,  $\Gamma_{1,cusp}$ , by the full cusp anomalous dimension,  $\Gamma_{cusp}$  of the interacting theory in question. So we can write

$$\langle W \rangle_{\tilde{U}(1)} = [\langle W \rangle_{U(1)}]_{\Gamma_{1,cusp}}^{\Gamma_{cusp}} = e^{\Gamma_{cusp} w_{U(1)}} \quad (3.5)$$

where  $w_{U(1)}$  is the result for a  $U(1)$  theory. This function is also related to the one loop maximally helicity violating amplitude once the tree level contribution is stripped out [19,10]. It is given by a single gluon (or rather photon) exchange between all pairs of lines. It is a completely explicit function of the distances between various cusps and we will not need its explicit expression<sup>5</sup>. The tilde in  $\tilde{U}(1)$  just reminds us that we have put the cusp anomalous dimension of the interacting theory.

---

<sup>4</sup> More precisely, they are the ratio of the expectation value with an insertion divided by the expectation value without the insertion.

<sup>5</sup> Its explicit form can be found in formula (4.58) of [10]. In this context this function is known as “the BDS expression”.

Thus the ratio

$$R = \log \left[ \frac{\langle W \rangle}{\langle W \rangle_{\tilde{U}(1)}} \right] \quad (3.6)$$

is a conformal invariant function. This is also called the remainder function. By definition, its first non-zero contribution is at two loops [13,6,14]. This definition clearly takes care of the divergence problem and leads to an explicitly conformal invariant answer. Though, this ratio takes care of the double logarithmic divergencies, there are single logarithmic divergencies that should be taken care of. These are regulator dependent. Thus, we adjust the regulator in the  $\tilde{U}(1)$  theory so that the single logarithmic divergencies match those of the full theory. Similarly there is a finite constant which is proportional to the number of cusps and is also regulator dependent <sup>6</sup>. These single log divergent terms or the constant terms are not important for this paper.

This ratio gives a nice conformal invariant expression, however, we should understand how it modifies the expectations from the point of view of the Hamiltonian interpretation of the family of polygons and the expansion for large  $\tau$ .

For this purpose, it is useful to note that  $\langle W \rangle_{\tilde{U}(1)}$  does have its own Hamiltonian interpretation since it is a computation in a  $U(1)$  theory. Thus, we have an expansion of the form in (3.2) where the anomalous dimensions vanish, and the energies appearing in (3.2) are simply the twist of the corresponding operators in the free  $U(1)$  theory. In the free  $U(1)$  theory the twists are just integers. Thus the expansion in (3.6) contains the ratio of the two expansions, or difference once we take the log.

In other words, the final version of the expansion takes the form

$$R = R^{\text{top}} + R^{\text{bottom}} + \int dn C_n e^{-E_n \tau + i p_n \sigma + i m_n \phi} - \int dn C_n^0 e^{-E_n^0 \tau + i p_n^0 \sigma + i m_n^0 \phi} \quad (3.7)$$

where the subindex 0 indicates that we are considering the  $U(1)$  theory.  $R^{\text{top}}$  and  $R^{\text{bottom}}$  are the remainder functions for the two polygons in figure fig. 5(b),(c). We are ignoring here a possible constant piece which is independent of the kinematics.

Now, in practice, we can distinguish the terms that come from the free theory because the energies are those of a free theory.

---

<sup>6</sup> We thank E. Sokatchev for pointing out the omission of these single logarithmic terms from the first version of this paper.



For example, if we consider the terms arising from a single insertion of the field  $F_{+i}$  then the expansion takes the simple form

$$R = R^{\text{top}} + R^{\text{bottom}} + \sum_{\pm} e^{\pm i\phi} \left[ \int dp C_{\pm}(p, \lambda) e^{-\epsilon(p, \lambda)\tau + ip\sigma} - e^{-\tau} \int dp C_{\pm}^0(p) e^{ip\sigma} \right] \quad (3.8)$$

The last term is the contribution from the  $U(1)$  theory and it has a simple  $\tau$  dependence. The first term includes the full dispersion relation and this leads to a more complicated  $\tau$  dependence. In the next section we will check that for the case of an hexagon the strong coupling answer [15], as well as the two loop weak coupling answer [13,20,21] has the form predicted by (3.8). We will also discuss the general structure of  $n$ -sided polygons at strong coupling. We see that (3.8) implies a particular structure for the Wilson loop correlator.

The dispersion relation  $\epsilon(p, \lambda)$  in (3.8) has been computed for all values of the coupling in [9]. Using that result, then (3.8) gives a prediction for the Wilson loop (or the MHV amplitude if they are equal) that should hold for all values of the coupling. Notice that we do not know what  $C$  is for all values of  $\lambda$ . Nevertheless we have a concrete prediction in terms of the  $\tau$  and  $\sigma$  dependence for the answer.

In appendix C we make further remarks on the spectrum of excitations around the flux tube. It would be useful for the reader to consult this appendix if he/she is not familiar with these excitations.

#### 3.4. Taking care of violations of conformal symmetry without using the $U(1)$ or one loop answer

It would be nice to be able to strip off completely the  $U(1)$  theory contribution from our expansion. This is actually possible, by regulating the anomalies in a different way. It is useful first to understand how this can be done in a  $U(1)$  theory. We start with the following ratio of Wilson loop expectation values in a  $U(1)$  theory.

$$r_{U(1)} = \log \left( \frac{\langle W \rangle_{U(1)} \langle W_{\text{square}} \rangle_{U(1)}}{\langle W^{\text{top}} \rangle_{U(1)} \langle W^{\text{bottom}} \rangle_{U(1)}} \right) \quad (3.9)$$

is finite and conformal invariant, if  $W^{\text{top}}$  is the Wilson loop with the bottom part replaced by the single bottom line of the square and  $W^{\text{bottom}}$  is the Wilson loop with the top part replaced by the single top line of the square, see fig. 5(b),(c).

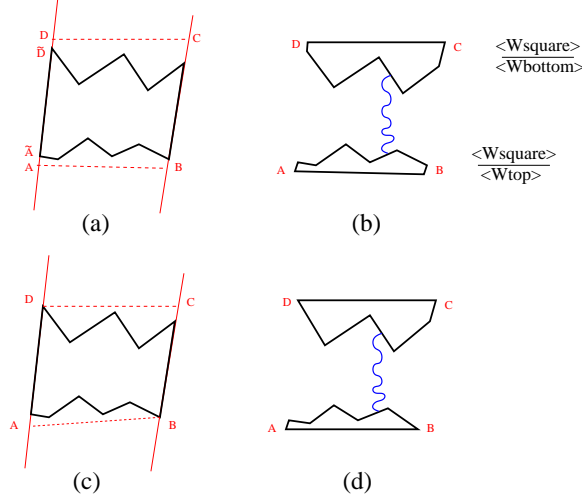


**Fig. 8:** (a) The original contour with the reference square given by its vertices  $ABCD$ . (b) The OPE expansion in the  $U(1)$  theory can be written in terms of  $r_{U(1)}$  which is computed by a single photon exchange between the top and bottom Wilson loops in this figure. In (c) and (d) we see the same, but with a choice of points that removes the divergencies. Points D and B of the reference square coincide with points on the original polygon.

The  $U(1)$  Wilson loop is the double integral of the free propagator

$$\log \langle W \rangle_{U(1)} = \frac{1}{2} \oint_W dx^\mu \oint_{W'} dx'^\nu G_{\mu\nu}(x, x') \quad (3.10)$$

where we regularized the integral by shifting  $W$  slightly in the second contour integral. Then it is easy to see that

$$r_{U(1)} = \oint_{W_{\text{square}} - W_{\text{top}}} dx^\mu \oint_{W_{\text{square}} - W_{\text{bottom}}} dx'^\nu G_{\mu\nu}(x, x') \quad (3.11)$$

Here the contours  $W_{\text{square}} - W_{\text{top}}$  and  $W_{\text{square}} - W_{\text{bottom}}$  are well separated and one is tempted to say that this expression is finite. However, there is a remaining divergence from propagators that connect the short portion of the null line in the bottom diagram with the segments that touch the extension of same null line in the top, see fig. 8. This leads to divergent terms that depend only on the location of the points along the null lines though  $AD$ , for example<sup>7</sup>. Such divergencies are independent of  $\sigma$ . They can be interpreted as

<sup>7</sup> There is a single log divergence proportional to the log of the cross ratio of the four points that are sitting along the null line passing through  $AD$ . In other words, we have a term  $\log \mu \log \frac{x_{AD}^2 x_{\tilde{A}\tilde{D}}^2}{x_{\tilde{A}D}^2 x_{A\tilde{D}}^2}$ , where  $AD$  are points on the reference square and  $\tilde{A}, \tilde{D}$  are points on the original polygon along the same line, see fig. 8(a). There a similar one from  $BC$ . These cross ratios depend only on  $\tau$  and not on  $\sigma$ . They vanish if  $D = \tilde{D}$  as in fig. 8(d).

coming from a condensate of Goldstone bosons of the broken  $SL(2, R)$  symmetry that acts on  $\tau$ . These divergencies can also be removed by choosing points B and D (or A and C) of the reference polygon to coincide with the vertices of the original polygon, see fig. 8(c) (d). Thus, we can either remove these divergencies by an appropriate choice of the reference polygon, or we can just simply ignore them because they are independent of  $\sigma$ .

The expansion of  $r_{U(1)}$  has the correct form to be identified with

$$r_{U(1)} = \int dn C_n^0 e^{-E_n^0 \tau + i p_n^0 \sigma + i m_n^0 \phi} \quad (3.12)$$

Indeed we can expand the propagator in eigenfunctions of the symmetries of the square, including the action of  $M$  on the bottom Wilson loop:

$$G_{\mu\nu}(x, x') dx^\mu dx'^\nu = \int dn dx^\mu \psi_\mu(x, n) dx'^\nu \psi_\nu(x', n) e^{-E_n^0 \tau + i p_n^0 \sigma + i m_n^0 \phi}$$

and compute the sources

$$c^{top}(n) = \oint_{W_{square} - W_{top}} dx^\mu \psi_\mu(x, n) \quad (3.13)$$

and  $c_{bottom}^0(n)$  so that  $c_n^0 = c_{top}(n) c_{bottom}(n)$ . In the next section we check this result for the hexagon Wilson loop. Note that this gives an explicit formula for the coefficients  $C^0 = \frac{\Gamma_{cusp}}{\Gamma_{1, cusp}} c_n^0$  appearing in the expansion (3.8).

With this  $U(1)$  result as an inspiration we are lead to define an alternative conformal invariant and finite expression<sup>8</sup>

$$r = \log \left[ \frac{\langle W \rangle \langle W_{square} \rangle}{\langle W_{top} \rangle \langle W_{bottom} \rangle} \right] \quad (3.14)$$

where now all expectation values are in the full interacting theory. This leads to a simple expansion involving only the physical excitations

$$r = \int dn C_n e^{-E_n \tau + i p_n \sigma + i m_n \phi} . \quad (3.15)$$

The combination in (3.14) is subtracting the contribution from the unexcited flux tube, or flux vacuum contribution. The remainder function defined in (3.6) is simply given by  $R = R_1 + R_2 + r - r_{\tilde{U}(1)}$ . Notice that the fact that (3.14) has an expansion in terms of subleading terms only also explains why the leading terms in the ordinary collinear limit are fixed by conformal symmetry. In that case  $W_{bottom}$  is a pentagon whose expectation value is fixed by the anomalous ward identities [11]. This pentagon leads to the terms in the splitting function computed previously [10].

---

<sup>8</sup> Again we choose  $D = \tilde{D}$  and  $B = \tilde{B}$  to eliminate a single log divergence. Alternatively, we could consider a more general reference square and ignore the  $\sigma$  independent divergence.

## 4. Detailed checks for the hexagon

A simple case that we can consider is the hexagonal Wilson loop. In this case there are three cross ratios  $u_1, u_2, u_3$ . Since our family involves three parameters, then it is clear that we can parametrize the three cross ratios in terms of the three parameters  $\tau, \sigma, \phi$ . In this case, the limit  $\tau \rightarrow \infty$  is a collinear limit which leaves behind a pentagon, which does not have any remaining cross ratios.

There are different ways to parametrize the  $u_i$ . An important choice is the choice of two opposite lines of the hexagon. There are three different ways of doing this which represent the three different channels in term of which we can expand the correlator. Once we chose a pair of opposite lines we can now choose the reference square in slightly different ways which amount to the action of the generators of  $SL(2, R)$  that leaves the two lines fixed. Different choices give slightly different parametrizations which only affect results at higher orders. These different choices change the answer in a predictable way, as is the case for the ordinary OPE. We can make a choice so that the cross ratios are, see appendix F.3,

$$\begin{aligned} u_2 &= \frac{1}{\cosh^2 \tau} \\ u_1 &= \frac{e^\sigma \sinh \tau \tanh \tau}{2(-\cos \phi + \cosh \tau \cosh \sigma)} \\ u_3 &= \frac{e^{-\sigma} \sinh \tau \tanh \tau}{2(-\cos \phi + \cosh \tau \cosh \sigma)} \end{aligned} \tag{4.1}$$

The expression for  $u_1$  and  $u_3$  appears rather complicated, but one may note that  $u_1/u_3 = e^{2\sigma}$  and that the parameter  $\mu$  appearing in the integral equations in [15] is  $\mu = -e^{i\phi}$ . In (2,2) signature we can set  $\mu = e^f$  and  $\cos \phi \rightarrow -\cosh f$ .

Once we have this parametrization we can expand the remainder function for large  $\tau$ .

### 4.1. Expansion of the hexagon at strong coupling

In this section we quote the result of the expansion of the hexagon at strong coupling. We leave the details to appendix F, where we show that the remainder function at strong coupling does indeed admit an expansion of the form (3.8) involving a reasonable spectrum of operators, thanks to the cancellation of several unwanted terms.

We expand the answer to order  $e^{-2\tau}$ . We find

$$\begin{aligned}
R &= R_1 + R_{\sqrt{2}} + R_2 + \dots \\
R_1 &= -\cos \phi e^{-\tau} (\cosh \sigma \log[2 \cosh \sigma] - \sigma \sinh \sigma) \\
R_{\sqrt{2}} &= 4 \cos \phi \int \frac{d\theta}{2\pi} \frac{1}{(\cosh 2\theta)^2} e^{-\tau\sqrt{2} \cosh \theta + i\sigma\sqrt{2} \sinh \theta} \\
R_2 &= e^{-2\tau} \left[ \frac{\log(2 \cosh \sigma) - \sigma}{2} + \cos 2\phi g(\sigma) \right] + 2 \int \frac{d\theta}{2\pi} \frac{e^{-2\tau \cosh \theta + 2i\sigma \sinh \theta}}{[\sinh(2\theta + i0)]^2}
\end{aligned} \tag{4.2}$$

Let us explain the interpretation of the various terms. The terms multiplied by  $\cos \phi$  correspond to the propagation of a particle created by the insertion of an excitation  $F_{+i}$  which carries unit charge under the transverse  $SO(2)$ . The  $R_1$  term has energy (or twist) one, independent of the momentum. This is then interpreted as coming from the  $U(1)$  subtraction term. The term  $R_{\sqrt{2}}$  is the contribution from the propagation of the corresponding particle at strong coupling. At strong coupling this particle has a relativistic dispersion relation with mass  $\sqrt{2}$ ; its momentum is  $p = \sqrt{2} \sinh \theta$ . The term  $R_2$  contains terms going like  $e^{-2\tau}$  which come from the contribution of the  $U(1)$  theory. One of them is independent of  $\phi$ . This term could come from the insertion of two twist one fields or one twist two field. The strong coupling contribution is again coming from the exchange of a single particle with a relativistic dispersion relation, last term in  $R_2$ . This particle has mass two. We do not know whether this particle remains present at all values of the coupling. It might decay into two fermions as it was found in a similar context in [22].

There is an interesting interplay between the terms with integer powers of  $e^{-\tau}$  and the integral terms. As we analytically continue  $\tau$  and  $\sigma$ , there are poles that cross the integration contours and we can get extra contributions which contain integer powers of  $e^{-\tau}$ . In fact, they combine with the terms already present to ensure that the expansion has the right properties. For example, the term in  $R_2$  going like  $e^{-2\tau}$  is not symmetric under  $\sigma \rightarrow -\sigma$ . This lack of symmetry is cured by the lack of symmetry of the integral which is introduced by the  $i0$  prescription. There are similar effects that occur when we go to large  $\sigma$  and then to  $\sigma > \tau$ . The result is invariant under the ‘‘Wick’’ rotation which exchanges  $\tau$  and  $\sigma$ .

#### 4.2. Expansion of the hexagon at weak coupling

When we expand (3.8) at weak coupling we generate terms going like  $\lambda^n \tau^k e^{-\tau}$ ,  $k \leq n - 1$ , where we took into account that  $C$  starts at order  $\lambda$ . These are the usual logs

that we get in perturbation theory and arise from the expansion of the exponent  $\epsilon(p, \lambda) = 1 + \lambda\gamma_1(p) + \dots$ , where  $\gamma_1(p)$  is the one loop anomalous dimension for the excitation. More concretely, consider the lowest order term, which is proportional to  $\cos \phi$ .

$$R = \cos \phi \int dp e^{ip\sigma} \left[ (\lambda C^{(1)} + \lambda^2 C^{(2)} + \dots) e^{-\tau - (\lambda\gamma_1 + \dots)\tau} - (\lambda + \lambda^2 \frac{\Gamma_2}{\Gamma_1}) e^{-\tau} c^0 \right] \quad (4.3)$$

where we have expanded everything in powers of  $\lambda$  and  $C^{(i)}$ ,  $c^0$  are functions of  $p$ .  $\Gamma_i$  are the coefficients in the expansion of the cusp anomalous dimension. Now, the fact that the remainder function is zero at order  $\lambda$  implies that  $C^{(1)} = c^0(p)$ , which is the result for the  $U(1)$  theory, or the result at one loop.

We can now compute the terms of order  $\lambda^2$ . Expanding (4.3) we find

$$R = \cos \phi e^{-\tau} \lambda^2 \int dp e^{ip\sigma} (C^{(2)} - \gamma_1 \tau c^0 + \frac{\Gamma_2}{\Gamma_1} c^0) \quad (4.4)$$

Thus, we can take the two loop expression and look at the term  $\tau e^{-\tau} h(\sigma)$ . If we fourier transform this term we get  $-\gamma_1(p) c^0(p)$ . We can independently compute  $c^0(p)$  from (3.13). We can also compute it with a trick: we can go to strong coupling, where the real result and the  $U(1)$  result do not mix. The  $U(1)$  result is contained in the term  $R_1$ . Its fourier transform is

$$c^0(p) \propto \int d\sigma e^{ip\sigma} (\cosh \sigma \log[2 \cosh \sigma] - \sigma \sinh \sigma) = \frac{1}{(1+p^2)} \frac{\pi}{\cosh \frac{p\pi}{2}} \quad (4.5)$$

It is easy to confirm this result from the direct expansion of  $r_{U(1)}$  in (3.11) at the leading order, see appendix D.

We also need to know  $\gamma_1(p)$ . This is given by the one loop anomalous dimension and for an  $F_{+i}$  propagating on a sea of derivatives. It was computed in [23] and is given by

$$\gamma_1(p) = \psi \left( \frac{3}{2} + i\frac{p}{2} \right) + \psi \left( \frac{3}{2} - i\frac{p}{2} \right) - 2\psi(1). \quad (4.6)$$

From [23] (equation (3.37) with  $s = 3/2$ ) we might naively expect  $-2\psi(3)$  instead of  $-2\psi(1)$ . However, we need to add the anomalous dimension per excitation  $\frac{\delta\Delta}{L\lambda} = 3$  of the state  $\text{tr} (F_{+i})^L$  [24] to the result of [23].

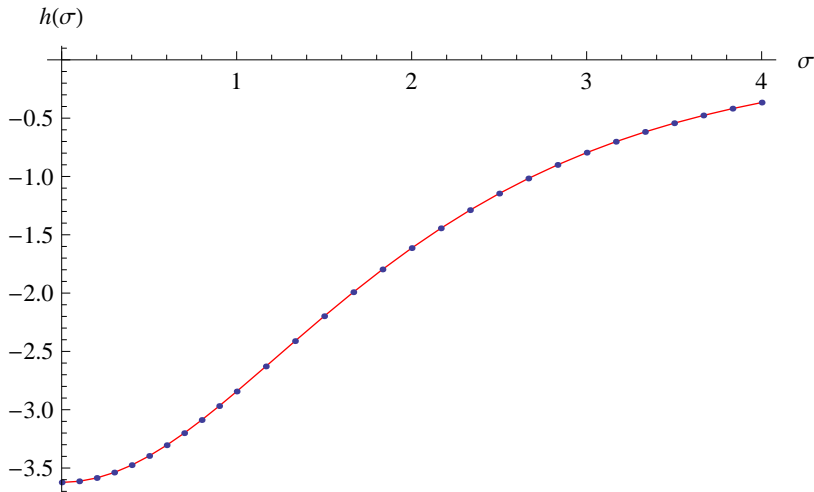


**Fig. 9:** Using the expressions from [21] we computed the functions  $h(\sigma)$  appearing in the expansion  $\tau e^{-\tau} h(\sigma)$  of the two loop result for the hexagon Wilson loop. The dots in this figure are the values obtained by fitting the numerical data in the large  $\tau$  regime. The red curve corresponds to the analytic prediction discussed in the main text. Recall that there is no fit of any parameter in this comparison; hence this check is a very strong check of our predictions.

We have checked numerically that this prediction is indeed true using the expressions from [21] for the two loop remainder function for the hexagon. In other words, the fourier transform of  $-\gamma_1(p)c^0(p)$  gives a function  $h(\sigma)$ <sup>9</sup> which is precisely the one appearing in the term  $\tau e^{-\tau} h(\sigma)$  in the expansion of the two loop result for large  $\tau$ , see figure fig. 9.

It should be clear that a similar prediction can be formulated for a general polygon, simply by replacing  $C^{(1)}(p)$  with the leading part of  $\log r_{U(1)}$  for that polygon. It would be interesting to check this prediction with an explicit two-loop calculation: the  $U(1)$  coefficient  $c^0(p)$  should capture the full, intricate dependence on the Wilson loop cross-ratios of the term  $\tau e^{-\tau} h(\sigma)$  in the expansion of the two loop result for large  $\tau$ .

Clearly, at higher loops we can make further predictions. For example, at  $l$  loops we expect that the remainder function has a term of the form

$$R \sim \cos \phi e^{-\tau} \frac{(-1)^{l-1} \tau^{l-1}}{(l-1)!} \int dp e^{ip\sigma} c^0(p) [\gamma_1(p)]^l \quad (4.7)$$

---

<sup>9</sup> This function can actually be computed analytically:

$$h(\sigma) \propto \cosh \sigma \left( 2 \log(1 + e^{2\sigma}) \log(1 + e^{-2\sigma}) - 4 \log(2 \cosh \sigma) \right) + 4\sigma \sinh \sigma$$

This is the highest power of  $\tau$  that appears at this loop order. We also have terms  $\tau^k e^{-\tau}$  with  $k < l - 1$ . These are also fixed by the knowledge of the dispersion relation at higher loops, which is given in [9].

## 5. Higher order predictions

In principle one can push the expansion of the remainder function to higher order in  $e^{-\tau}$ , and consider terms which correspond to the propagation of several particles. The states which appear in the  $U(1)$  answer  $C_n^0$  are naively only “one particle states”, corresponding to insertions of a single four dimensional field on the sea of derivatives. At the 1-loop, in the spin chain language, such naive “one particle states” will mix with the continuum of true multi-particle excitations, and possibly to actual single particle bound states. Even without computing the exact 1-loop overlaps, we still get some constraints on terms of the form  $\tau e^{-k\tau} H(\sigma)$  in the expansion of the two loop result of a general polygon for large  $\tau$ , at least as long as  $k$  is sufficiently small compared to the number of sides of the polygon: the full functional dependence of  $H(\sigma)$  on the cross-ratios is captured by the twist  $k$  coefficients  $C_k^0(p) = C_k^{0\text{top}} C_k^{0\text{bottom}}$ , multiplied by some unknown function of  $p$  which does not depend on the specific shape of the top and bottom Wilson loops.

## 6. Conclusions

In this paper we have derived an OPE expansion for polygonal Wilson loops with light-like edges. The OPE expansion is performed by picking two non-consecutive null lines in the polygonal Wilson loop. This divides the Wilson loop into a “top” part and a “bottom” part with states propagating between the two. The state that propagates contains a flux tube going between the two selected null lines. The states consist of excitations of this flux tube. These states can also be understood as excitations around high spin operators. The spectrum of states is continuous and consist of many particles propagating along the flux tube. In  $\mathcal{N} = 4$  Super Yang Mills these particles have a calculable dispersion relation [9]. Then the OPE expansion leads to predictions for the Wilson loop expectation values. Namely, it implies constraints on the subleading terms in the collinear limit of the remainder function, which is the function containing the conformal invariant information of the Wilson loop expectation value. We have checked these predictions both at strong coupling and at two loops at weak coupling.



In order to perform this expansion at strong coupling, we have derived an alternative presentation of the integral equations [25,15,16]. In the new representation the parameters in the equations are the physical spacetime cross ratios. In addition, the formula for the area is given by the Yang-Yang functional associated to the modified TBA equations. This new form of the equations are as useful as the old ones [25,15,16] for numerical computations.

For single particle exchanges we have been able to characterize completely the state of the particle in terms of its momentum. Using the exact formula for the single particle dispersion relation, given in [9], one can find an exact prediction for the first subleading term in the collinear expansion. Expanding this formula in powers of  $\lambda$  one would obtain specific predictions to all orders. Here we have checked this prediction with the only available direct computation in the literature, the two loop hexagon [13,6,14,20,21].

When we have multiparticle exchanges the situation is less clear and we will probably need the full power of integrability, together with the infinite number of charges to characterize the state. It is likely that characterizing the states in this fashion and then demanding a consistent expansion in all channels one could determine the full function.

## 7. Acknowledgments

We thank Benjamin Basso for discussions and for providing us with a draft of [9]. We also thank N. Arkani-Hamed, F. Cachazo, P.Dorey, M. Spradlin, D.Volin and K.Zarembo for discussions.

This work was supported in part by U.S. Department of Energy grant #DE-FG02-90ER40542. Research at the Perimeter Institute is supported in part by the Government of Canada through NSERC and by the Province of Ontario through MRI. D.G. is supported in part by the Roger Dashen membership in the Institute for Advanced Study. D.G. is supported in part by the NSF grant PHY-0503584. A.S. and P.V. thanks the Institute for Advanced Studies for warm hospitality. J.M. thanks the Perimeter Institute for hospitality.

## Appendix A. Describing the family of polygons in terms of momentum twistors

One can describe the kinematics of the family of polygons that we considered in section 3.1 by twistors. These are sometimes called “momentum twistors” and they appear naturally both in weak coupling [26] and strong coupling [25,15,16] calculations.

Each vertex of the polygon can be represented by a null vector  $Z$  in  $R^{4,2}$ , defined up to rescaling. The vector  $Z$  can be thought of carrying two antisymmetric spinor indices, and can be rewritten as the bilinear antisymmetric combination of two twistors. Schematically,  $Z = \lambda \wedge \lambda'$ . Both  $\lambda$  and  $\lambda'$  carry a spinor index of  $R^{4,2}$  and are defined up to rescaling. A polygon with  $N$  null sides can be given as a sequence of  $N$  twistors  $\lambda_i$ , such that the intersection of the sides  $i$  and  $i+1$  is the point  $Z_{i+1/2} = \lambda_i \wedge \lambda_{i+1}$ . Indeed  $Z_{i-1/2} \cdot Z_{i+1/2} = 0$  is the condition that the  $i$ -th side should be null. It is also useful to introduce dual momentum twistors  $\mu_i$ , cospinors which can be defined as  $\mu_i = \lambda_{i-1} \wedge \lambda_i \wedge \lambda_{i+1}$ , and also satisfy  $Z_{i+1/2} = \mu_i \wedge \mu_{i+1}$ .

A twistor  $\lambda$  together with an orthogonal dual twistor  $\mu$ ,  $(\mu, \lambda) = 0$ , defines a null line (and viceversa): all points of the form  $Z = \lambda \wedge v$  with  $(\mu, v) = 0$ ,  $v$  defined up to rescaling and shifts by  $\lambda$ . Our family of polygons with fixed sides  $i, j$  must have fixed  $\lambda_{i,j}$  and  $\mu_{i,j}$ . We are now in condition to give an alternative description of the group of transformations fixing two non-intersecting null lines, defined by the pairs  $\lambda_i, \mu_i$  and  $\lambda_j, \mu_j$ . In order for the lines to be at generic position with respect to each other,  $(\mu_i, \lambda_j)$  and  $(\mu_j, \lambda_i)$  should be both non-zero. A conformal transformation  $M$  will leave the lines invariant if  $\lambda_{i,j}$  are right eigenvectors of  $M$ , i.e.  $M\lambda_i = e^{\sigma+\phi}\lambda_i$  and  $M\lambda_j = e^{-\sigma+\phi}\lambda_j$ , and  $\mu_{i,j}$  are left eigenvectors. As long as  $(\mu_i, \lambda_j)$  and  $(\mu_j, \lambda_i)$  are non-zero, it must be that  $\mu_i M = \mu_i e^{-\sigma+\phi}$  and  $\mu_j M = \mu_j e^{\sigma+\phi}$ .

If we decompose the twistor space into multiples of  $\lambda_i$ , multiples of  $\lambda_j$  and the orthogonal to  $\mu_{i,j}$ ,  $M$  will be block diagonal, with elements  $e^{\pm\sigma+\phi}$  and  $e^{-\phi}R$  for some  $SL(2)$  transformation  $R$ . To pick a reference square is the same as picking two more twistors  $\lambda_{\pm}$  in the orthogonal to  $\mu_{i,j}$ . The square is left invariant by  $M$  iff  $\lambda_{\pm}$  are the two remaining eigenvectors of  $M$ , with eigenvalues  $e^{\pm\tau-\phi}$ .

Once we have picked a specific reference square, the family of polygons is defined by the twistors  $\lambda_i \cdots \lambda_j$  and  $M\lambda_{j+1} \cdots M\lambda_{i-1}$ .

## Appendix B. The hamiltonian picture and its analytic continuation

In this appendix we consider the large spin limit of local operators and we see how they give rise to the flux vacuum and its excitations.

We write the coordinates of  $R^{1,3}$  as  $Z_M = Z_{-1}, Z_0, Z_1, \cdots Z_4$ , with the condition  $Z^2 = 0$ , where the indices are contracted with the Minkowski metric of  $R^{2,4}$ . In addition we impose the identification  $Z \sim \lambda Z$ . Usual poincare coordinates are

$$x_{\mu} = \frac{Z_{\mu}}{(Z_{-1} + Z_4)}, \quad \text{for } \mu = 0, 1, 2, 3 \quad (\text{B.1})$$

The usual  $R^{1,3}$  metric is simply the induced metric on the lightcone  $Z^2 = 0$  with the gauge condition  $Z_{-1} + Z_4 = 1$ . Different “gauge fixing” conditions lead to Weyl transformations for the metric. Just for reference, the usual coordinates of  $R \times S^3$  are defined by

$$\tan t = \frac{Z_0}{Z_{-1}}, \quad n^i = \frac{Z^i}{\sqrt{\sum_{i=1}^4 Z_i^2}}, \quad i = 1, \dots, 4 \quad (\text{B.2})$$

where  $n^i$  is a unit vector in  $R^4$  and describes a point on  $S^3$ . Similarly, if we choose a gauge fixing function  $Z_2^2 + Z_3^2 = 1$  we get a metric which is that of  $AdS_3 \times S^1$ .<sup>10</sup> This is again conformally related to  $R^{1,3}$ .

Within this  $AdS_3$  factor we can choose coordinates which are similar to Euler angles for  $S^3$  (since  $AdS_3$  is an analytic continuation of  $S^3$ ). We can write

$$Y^M = \frac{Z^M}{\sqrt{Z_2^2 + Z_3^2}}, M \neq 2, 3; \quad \begin{pmatrix} Y_{-1} + Y_4 & Y_0 + Y_1 \\ -Y_0 + Y_1 & Y_{-1} - Y_4 \end{pmatrix} = e^{i\tau_1 \sigma_2} e^{\beta \sigma_3} e^{\sigma \sigma_1} \quad (\text{B.3})$$

where  $\sigma_i$  are the usual Pauli matrices. We have parametrized the space in terms of coordinates  $\tau_l, \beta, \sigma$  and  $\phi = \arctan(Z_2/Z_3)$ . The metric in these coordinates is

$$\begin{aligned} ds_{AdS_3 \times S^1}^2 &= -d\tau_l^2 + d\sigma^2 + d\beta^2 + 2 \sinh 2\beta d\tau_l d\sigma + d\phi^2 = \\ &= (d\sigma + \sinh 2\beta d\tau_l)^2 - \cosh^2 2\beta d\tau_l^2 + d\beta^2 + d\phi^2 \end{aligned} \quad (\text{B.4})$$

These coordinates make manifest the symmetries of the two Wilson line configuration. We see that the  $\sigma$  direction is fibered over an  $AdS_2$  space which realizes the  $SL(2, R)$  symmetry. This metric differs from the flat metric of  $R^{1,3}$  by an overall conformal factor, which is not important if we are dealing with a conformal field theory. We can consider two Wilson lines at  $Z_2 = Z_3 = 0$  and at  $Z_0/Z_{-1} = Z_1/Z_4$ . The  $SL(2, R)$  that preserves two of the lines acts by multiplication on the left in (B.3). These Wilson lines lie at the boundary of the  $AdS_3$  space and produce a flux of color electric field along the  $\tau_l, \sigma$  directions,  $F_{\tau_l \sigma} = \text{constant}$ . This is a flux tube whose energy is localized in the transverse non-compact  $\beta$  direction. This is discussed in more detail in [18]. Excitations of this flux vacuum constitute the states that arise in the OPE expansion. In any theory where the flux cannot “break”, these states are well defined. For example, in  $\mathcal{N} = 4$  super Yang Mills

---

<sup>10</sup> This  $AdS_3$  has no relation to the  $AdS$  space that appear in  $AdS/CFT$ . This  $AdS$  space is purely within the boundary theory. This discussion applies to any CFT, whether it has a known gravity dual or not.

this flux is well defined at finite  $N$  for any value of the coupling if the external lines are in the fundamental, so that the flux cannot be screened. In theories with fundamentals, these states might be not defined away from the planar limit.

Let us now discuss the analytic continuation  $\tau_l \rightarrow i\tau$ . We also need to set  $\beta \rightarrow i\tilde{\beta}$ . Then the coordinates (B.3) continue to describe an  $AdS_3$  space written as an  $SU(1,1)$  group element where we have analytically continued  $Y_4 \rightarrow iY_0$  and  $Y_0 \rightarrow iY_4$ . This now maps the Wilson lines as follows. After the analytic continuation the parametrization (B.3) becomes a parametrization as an  $SU(1,1)$  matrix. We can perform a simple relabeling of the matrices  $\sigma_2 \rightarrow \sigma_3$  and  $\sigma_3 \rightarrow -\sigma_2$  which corresponds to the transformation which takes the  $SU(1,1)$  group element back to the usual presentation in terms of  $SL(2, R)$  matrices. After this transformation we end up with a parametrization of the form

$$\begin{pmatrix} \tilde{Y}_{-1} + \tilde{Y}_4 & \tilde{Y}_0 + \tilde{Y}_1 \\ -\tilde{Y}_0 + \tilde{Y}_1 & \tilde{Y}_{-1} - \tilde{Y}_4 \end{pmatrix} = e^{\tau\sigma_3} e^{i\tilde{\beta}\sigma_2} e^{\sigma\sigma_1} \quad (\text{B.5})$$

We now see that the transformation  $\tau \rightarrow \tau + \text{constant}$  corresponds to a combination of an ordinary dilatation and a boost if we go back to the usual Poincare coordinates via (B.1). This is such that it leaves  $x^+$  fixed and it changes  $x^-$ . We then get a square as in fig. 4(c). The two original Wilson lines are the ones acted on by these shifts of  $\tau$  and are the ones that are extended along  $x^-$ . The other two sides of the square have arisen after the analytic continuation and they are the lines on which are inserting the operators creating the flux vacuum together with its excitations. If we only have the flux vacuum, these extra lines do not have any further operators inserted. See also fig. 6(b).

### B.1. Analytic continuation at strong coupling

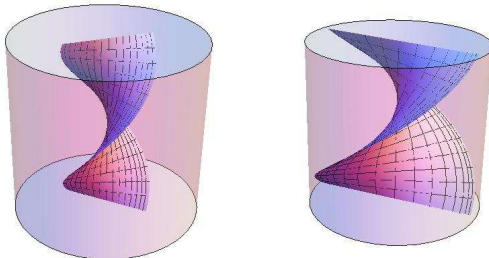


**Fig. 10:** Plot of the the spinning string solution for small spin and for large spin.

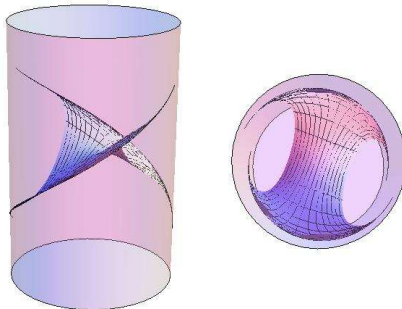


**Fig. 11:** Plot of the Euclidean continuation of the spinning string solution for small spin. Side view and top view.

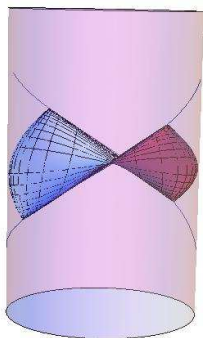


**Fig. 12:** Plot of the Euclidean continuation of the spinning string solution for very large spin. The edges of the string in the bulk approach the boundary, leading to the two other boundaries of the Wilson loop.

At strong coupling we can consider the string solution that is dual to the high spin operators considered in [7]. In this appendix we will show how the high spin limit, plus an analytic continuation, produces the square Wilson loop. A closely related discussion can be found in [27]. The idea that the large spin limit can be described in terms of Wilson loops can be found in [28]. It is convenient to focus just on an  $R^{1,1}$  subspace of the boundary theory and an  $AdS_3$  subspace of the bulk, with metric  $ds^2 = -\cosh^2 \rho dt^2 + \sinh^2 \rho d\varphi^2 + d\rho^2$ . This should not be confused with the  $AdS_3$  subspace discussed above which was purely on the boundary. For finite spin we have the solution [7]

$$\varphi = wt, \quad \rho \in [0, \rho_{max}], \quad \tanh \rho_{max} = 1/w \quad (\text{B.6})$$

where  $w$  is very large for small spin and  $w \rightarrow 1$  when the spin goes to infinity. This is the Lorentzian time solution. We can now analytically continue  $t \rightarrow i\tau$  and  $\varphi \rightarrow i\chi$ . We then

write

$$\tilde{Y}_{-1} \pm \tilde{Y}_4 = e^{\pm\tau} \cosh \rho, \quad \tilde{Y}_0 \pm \tilde{Y}_1 = e^{\pm w\tau} \sinh \rho, \quad \rho \in [0, \rho_{max}] \quad (\text{B.7})$$

This is plotted in fig. 11. We see that as we approach the boundary and  $\tau \rightarrow \infty$  the solution approaches two null lines. The worldsheet tips, sitting at  $\rho = \rho_{max}$ , move through the bulk and approach the boundary along these null lines. As the spin goes to infinity  $w \rightarrow 1$  and  $\rho_{max} \rightarrow \infty$ . Then the tips of the string get closer to the boundary. In the limit, the tip is joining a point that is a quarter way from the tip of the null line in fig. 11 to a light-like separated point on the other line.

At weak coupling we expect a similar picture. In fact, a closely related picture was discussed in [28]. The insertion of an operator  $Tr[\Phi\partial_{\pm}^S\Phi]$  produces a displacement of the field insertions along the  $x^+$  direction together with an adjoint Wilson line.<sup>11</sup> As the spin gets larger we expect that the effective displacement of the two fields along the null direction becomes larger. Now suppose that we have two such operators inserted at antipodal points in the cylinder. These points are spacelike separated. However, as we increase the spin, each of the points is splitting into two and they become displaced along the null direction. As this displacement grows one of the  $\Phi$  insertions of one operator can become light-like separated with the  $\Phi$  insertion of the other. This happens as the spin goes to infinity. Operators that diagonalize the dilation do not have fixed separation along the  $x^+$  direction, but are a suitably weighted superposition. At strong coupling this manifests itself as the fact that we always get full null lines as we approach  $\tau \rightarrow \pm\infty$  in (B.7), see fig. 11.

This picture is not restricted to the large spin limit of twist two operators, but it would also hold for higher twist operators which contain other field insertions among the derivatives, as long as we consider the large spin limit and look at the lowest excitations. See [17] for further discussion and further references.

Finally, notice that by inserting  $n$  high spin twist two operators at spacelike separated points and by taking their large spin limit we expect to reproduce a null polygonal Wilson loop with  $2n$  sides. In particular, the three point function of high spin operators of the type  $Tr[\Phi\partial^S\Phi]$  should produce the hexagonal Wilson loop, when each of the spins goes to infinity. The cross ratios of the Wilson loop should come from the orientation of the spins and their ratios as they go to infinity. It should be interesting to see if this produces a simpler way to compute Wilson loop expectation values.

---

<sup>11</sup> Alternatively, a null Wilson line between two  $\Phi$  insertions can be expanded in derivatives. Then, correlators of these Wilson operators are dominated by large spin.

### Appendix C. Remarks on the dispersion relation

In this appendix we would like to make a couple of remarks on the dispersion relation for excitations around the flux vacuum described in the above appendix. Let us discuss it first at weak coupling. In the free theory, the particles do not feel the flux and the spectrum is the same as in the absence of flux. It turns out that the energies are quantized and independent of the momentum, due to the  $SL(2, R) \times SL(2, R)$  representation theory of the problem [18]. At first order in the coupling we get a correction. The states in question can be viewed as excitations around an infinite “sea of derivatives”. In other words, high spin operators have the rough form  $Tr[\Phi \partial_+^S \Phi]$ . In the large  $S$  limit, the two field insertions  $\Phi$  become displaced by the derivatives giving rise to the Wilson lines. Thus, we are left with the sea of derivatives. We can then insert other fields among this sea of derivatives. In the free theory the total twist, which we are calling “energy”, is just the twist of the extra fields, which could be 1,2,3, etc. At first order in the coupling we see that the degeneracy is broken and we get a non-trivial dispersion relation. A similar phenomenon occurs around other large charge “vacua” such as the BMN vacuum [29]. At one loop the twist one fields give rise to well defined excitations with a dispersion relation  $\epsilon(p) = 1 + \lambda\gamma(p)$ . For  $\mathcal{N} = 4$  SYM these excitations are two gauge field insertions  $F_{+i}$  and six scalars  $\Phi^I$ , and eight fermionic excitations  $\psi_{+\frac{1}{2},\alpha}$ . Since these fields are well defined particles at weak coupling, we expect that they will survive at all values of the coupling. At twist two we have several possibilities, one of them is  $F_{+-}$ , for example. We do not know if it survives as a well defined particle for all values of the coupling. At strong coupling we have an accidental relativistic symmetry, as we have around the BMN vacuum [29]. This is only present at strong coupling and is broken as we go away from the strong coupling limit. We have [30] particles with mass  $m = \sqrt{2}$  that corresponds to the  $F_{+i}$  particles. We also have eight massive fermions of mass  $m = 1$ . We have five massless scalars from the five sphere. Due to strong IR effects these give rise to six massive particles of very tiny mass  $m \propto e^{-\frac{1}{4}\sqrt{\lambda}}$  [18]. Finally, there is a particle of mass  $m = 2$ .

It turns out that some of these particles can be interpreted as “massive goldstone” particles.

Notice that after the analytic continuation in (B.5) the coordinates (B.4) become

$$ds^2 = d\tau^2 + d\sigma^2 + 2 \sin \tilde{\beta} d\tau d\sigma - d\tilde{\beta}^2 + d\phi^2 \quad (\text{C.1})$$

We see that we have a symmetry under  $\tau \leftrightarrow \sigma$  and  $\tilde{\beta} \rightarrow -\tilde{\beta}$ . This leaves the flux essentially invariant. This implies that the dispersion relation is expected to have the following symmetry. If we write the dispersion relation as  $f(\epsilon, p, \lambda) = 0$ , then if  $\epsilon$  and  $p$  are a solution, then so is  $\epsilon' = ip, p' = i\epsilon$ . Thus we have a Wick rotation symmetry.

### C.1. Massive Goldstone particles

The flux vacuum that we are considering in this paper is breaking some symmetries spontaneously. When we have spontaneously broken symmetries we can act with the broken symmetry generators and generate some particular excitations. These excitations have particular energies and momenta which are fixed by the commutation relations between the broken symmetry generator and the energy and momentum generators. Let us see what this implies for our case [18]. For example, the flux breaks supersymmetry. Under the  $SL(2)_L \times SL(2)_R \subset SO(2,4)$  generators the supercharges transform as  $(\frac{1}{2}, 0) + (0, \frac{1}{2})$ . Thus they have either  $\epsilon = \pm 1$  and  $p = 0$  or  $\epsilon = 0$ ,  $p = \pm i$  (recall that the energy is a generator inside  $SL(2)_L$  and the momentum is a generator inside  $SL(2)_R$ ). Thus the dispersion relation of the fermions should obey

$$\epsilon(\lambda, p = 0) = 1 \quad , \quad \epsilon(\lambda, p = \pm i) = 0 \quad , \quad \text{fermions} \quad (\text{C.2})$$

This should be true for all values of the coupling. E.g., this argument determines the mass of the fermions at strong coupling.

For the bosons associated to  $F_{+i}$  there is a similar prediction. In this case the corresponding generators have spin  $(\frac{1}{2}, \frac{1}{2})$  under the  $SL(2) \times SL(2)$  of  $AdS_3$ . Thus, in this case the Goldstone bosons have  $\epsilon = \pm 1$ ,  $p = \pm i$ . Thus, in this case we have the constraint

$$\epsilon(\lambda, p = \pm i) = 1 \quad , \quad F_{+i} \quad \text{bosons} \quad (\text{C.3})$$

One is tempted to make the same argument for the broken generator involving the broken  $SL(2, R)$  generators. In this case one would be lead to a particle with energy  $\epsilon = 2$ ,  $p = 0$ . This is indeed present at strong coupling, it is the  $m = 2$  particle. On the other hand, it might be that this particle decays into pairs of fermions, which would mean that the symmetry generator would create pairs of fermions rather than a single boson. Notice that the prediction (C.3) is quite general. It should hold in any CFT in dimensions  $d \geq 3$ . Superficially this relation seems to be contradicted by (4.6); we believe that the limit  $p \rightarrow i$  does not commute with perturbation theory. A closer analysis of the finite coupling dispersion of [9] should hopefully confirm this.

This non-relativistic version of the Goldstone theorem constrains the dispersion relation only at particular values of the momentum. In these cases the broken symmetries do not commute with the Hamiltonian and thus they give rise to excitations with finite energies.

Notice that the excitations around the flux vacuum have a gap, both at weak and strong coupling, though the gap becomes non-perturbatively small at strong coupling. In particular, the anomalous dimensions of the  $\Phi^J$  insertions at zero momentum is negative, as naively expected from the fact that they become very small at strong coupling [23,9].



## Appendix D. On the expansion for Wilson loops in the $U(1)$ theory

In this appendix we aim to give some more details about the computation of  $r_{U(1)}$  for a general polygon. It is convenient to rewrite the contour integrals in terms of projective coordinates  $Z$  as

$$\log r_{U(1)} = \oint_{\substack{W_{square} - \\ W_{top}}} ds \oint_{\substack{W_{square} - \\ W_{bottom}}} ds' \frac{\dot{Z}(s) \cdot \dot{Z}'(s')}{Z(s) \cdot Z'(s')} \quad (\text{D.1})$$

Notice that a position-dependent real rescaling  $Z(s) \rightarrow Z(s)\lambda(s)$  changes the integrand up by a total derivative only, which integrates to zero. Be  $A, D$  the top vertices of the square,  $B, C$  the bottom vertices.  $W_{square} - W_{top}$  consists of a path  $\gamma$  going from  $A$  to  $D$  minus the straight segment  $AD$ , see fig. 8(b).  $W_{square} - W_{bottom}$  consists of a path  $\gamma'$  going from  $B$  to  $C$  minus the straight segment  $BC$ . We can write  $\gamma(s) = a(s)A + b(s)B + c(s)C + d(s)D + n(s)$ , where  $a, b, c, d$  are scalar functions and  $n$  is a vector in the plane orthogonal to the square. We can also write  $\gamma'(s') = a'(s')A + b'(s')B + c'(s')C + d'(s')D + n'(s')$ . It is useful to parameterize the segment  $AD$  as  $Z_0(s) = a(s)A + d(s)D$  and write  $\gamma(s) = Z_0(s) + \delta(s)$ . Without loss of generality, we can pick  $a(s) = e^{-s}$  and  $d(s) = e^s$ . We will also parameterize the segment  $BC$  as  $Z'_0(s') = b'(s')B + c'(s')C$  and write  $\gamma'(s') = Z'_0(s') + \delta'(s')$ . Without loss of generality, we can pick  $b'(s') = e^{-s'}$  and  $c'(s') = e^{s'}$ . We can also normalize  $A \cdot C = B \cdot D = 1/2$ .

Notice that  $\delta \cdot Z' = \delta' \cdot Z = 0$  and their derivatives are also orthogonal. After some simple algebra

$$\log r_{U(1)} = \int_{-\infty}^{\infty} ds \int_{-\infty}^{\infty} ds' \frac{\delta(s) \cdot \delta'(s') + \dot{\delta}(s) \cdot \dot{\delta}'(s')}{\cosh(s - s') + \delta(s) \cdot \delta'(s')} \quad (\text{D.2})$$

The action of  $M$  on  $\gamma'(s')$  can be combined with a trivial rescaling and shift of the integration variable as  $e^{-\tau} M \gamma'(s' - \sigma) = e^{-2\tau - \sigma} a'(s' - \sigma)A + e^{-s'} B + e^{s'} C + e^{-2\tau + \sigma} d'(s' - \sigma)D + e^{-\tau} n'_\phi(s' - \sigma)$ . We denoted the action of the rotation in the transverse plane on  $n'$  as  $n'_\phi$ . Hence in order to write the OPE we want to redefine  $\delta'(s' - \sigma, \tau, \sigma, \phi) = e^{-2\tau - \sigma} a'(s' - \sigma)A + e^{-2\tau + \sigma} d'(s' - \sigma)D + e^{-\tau} n'_\phi(s' - \sigma)$ , and

$$\log r_{U(1)} = \int_{-\infty}^{\infty} ds \int_{-\infty}^{\infty} ds' \frac{\delta(s) \cdot \delta'(s' - \sigma) + \dot{\delta}(s) \cdot \dot{\delta}'(s' - \sigma)}{\cosh(s - s') + \delta(s) \cdot \delta'(s' - \sigma)} \quad (\text{D.3})$$

Now we can expand the denominator and Fourier transform term by term. The leading piece is

$$\begin{aligned} \log r_{U(1)} &\sim e^{-\tau} \int_{-\infty}^{\infty} ds \int_{-\infty}^{\infty} ds' \frac{n(s) \cdot n'_\phi(s' - \sigma) + \dot{n}(s) \cdot \dot{n}'_\phi(s' - \sigma)}{\cosh(s - s')} \sim \\ &\sim \int dp e^{ip\sigma - \tau} \tilde{n}(p) \cdot \tilde{n}'_\phi(p) \frac{p^2 + 1}{\cosh \frac{\pi p}{2}} \end{aligned} \quad (\text{D.4})$$

For the hexagon we find that  $n(s) \sim e^{-|s|} n_0$  where  $n_0$  is a constant vector. We have a similar expression for  $n'$ . Its Fourier transform is then proportional to  $(1 + p^2)^{-1}$ . We get a similar factor from  $n'$ . Together these two factors give the function in (4.5).

## Appendix E. The modified TBA and Yang-Yang functional for $AdS_3$ null polygons

In this appendix we present a new version for the integral equations that determine the result at strong coupling in the case that the polygon can be embedded in  $R^{1,1}$  and the surface in  $AdS_3$ . This modified integral equations, or TBA equations, involve only the physical spacetime cross ratios, in contrast with the ones in [16] which involved some other auxiliary parameters. In addition, we will find that the expression for the area can be written as the critical value of the associated Yang-Yang functional [31,32]. The computation of the regularized area (or better, the remainder function) for the minimal surface in  $AdS_3$  ending on a given null polygon on the boundary is done in [25,16] through three basic steps. The first step is to promote the cross-ratios of the null polygon to holomorphic functions of a spectral parameter  $\zeta$ , which capture the higher conserved charges of the classical integrable system. The second step is to derive a set of functional equations, which are then converted into convenient integral equations. The third step is to compute the regularized area from the higher conserved charges or  $\zeta$  dependent cross ratios.

The specific problem of minimal surfaces ending on null polygons in  $AdS_3$  is a special case of a general theory of Hitchin systems on a Riemann surface. The results of this appendix apply to any such system, hence we will try to keep our integral equations as general as possible. Fortunately, the integral equations given for general Hitchin systems [33,34] and the integral equations which are optimized for the case of polygons in  $AdS_3$  [16] actually coincide in the simplest kinematic region. There is a large amount of freedom in setting up the Riemann Hilbert problem, which leads to a variety of different forms for

the integral equations, each with its own advantages and disadvantages. The purpose of this appendix is to present the integral equations in a way which is well suited for the analysis of soft limits, and make manifest the cancellation of spurious terms between the various contributions to the regularized area.

The TBA-like integral equations for general Hitchin systems can be written as

$$\ln X_\gamma(\zeta) = \frac{Z_\gamma}{\zeta} + i\theta_\gamma + \bar{Z}_\gamma\zeta - \frac{1}{4\pi i} \sum_{\gamma' \in \Gamma} \Omega(\gamma') \langle \gamma, \gamma' \rangle \int_{\ell_{\gamma'}} \frac{d\zeta'}{\zeta'} \frac{\zeta' + \zeta}{\zeta' - \zeta} \log(1 + X_{\gamma'}(\zeta')) \quad (\text{E.1})$$

The equations depend on some discrete data: the set  $\Gamma$  of possible labels  $\gamma, \gamma'$ , certain integer numbers  $\Omega(\gamma)$ , an antisymmetric pairing  $\langle \gamma, \gamma' \rangle$ . This data is the final product of a careful WKB analysis of some differential equations on the surface, and for the purpose of this appendix we only need to use some basic facts about it. The  $Z_\gamma$  are auxiliary complex numbers which we wish to eliminate from the equations. The  $\theta_\gamma$  are angles which will presently be set to zero (or  $\pi$ , in which case they can be reabsorbed by changing the sign of some  $X_\gamma$  in the equations): in the language of Hitchin systems, we are restricting to a real section. The lines of integration  $\ell_\gamma$  are straight rays from  $\zeta' = 0$  to  $\zeta' = \infty$ , which for convergence reasons should lie in the half plane where  $Z_\gamma/\zeta'$  has a negative real part. A canonical choice is to set them to  $Z_\gamma/\zeta'$  real and negative. The relative ordering of the lines is important, in the sense that if two lines are moved across each other, the integration contours will cross poles of the integration kernels. The result of such a “wallcrossing” is captured by a certain specific change in the discrete data.

Once the angles  $\theta_\gamma$  are set to zero, a simplification occurs:  $X_{-\gamma}(-\zeta) = X_\gamma(\zeta)$ . This is due to a certain symmetry of the equations: labels in  $\Gamma$  come in pairs, which we can denote as  $\gamma$  and  $-\gamma$ , such that  $\Omega(\gamma) = \Omega(-\gamma)$ ,  $\langle -\gamma, \gamma' \rangle = \langle \gamma, -\gamma' \rangle = -\langle \gamma, \gamma' \rangle$ ,  $Z_{-\gamma} = -Z_\gamma$ .

We can combine the contributions from  $\gamma'$  and  $-\gamma'$ , and have the sum run only half of the set of  $\gamma$ 's, say  $\Gamma^+$ . From now all sums will be over this subset. We will also write  $\zeta = e^\theta$ .

$$\ln X_\gamma(\theta) = Z_\gamma e^{-\theta} + \bar{Z}_\gamma e^\theta + \frac{1}{2\pi i} \sum_{\gamma' \in \Gamma^+} \Omega(\gamma') \langle \gamma, \gamma' \rangle \int_{\ell_{\gamma'}} \frac{d\theta'}{\sinh(\theta' - \theta)} \log(1 + X_{\gamma'}(\theta')) \quad (\text{E.2})$$

In order to make contact with the equations of [16] for  $2N$  gluons we can take the labels  $\gamma = s$  to run over integers  $1 \cdots N - 3$ , with  $\Omega(s) = 1$  and  $\langle s, s + 1 \rangle = -1$ . We also

need to set  $Z_s = -\frac{i^s}{2}m_s$ , and use the canonical choice of lines. The functions  $X_s$  and  $Y_s$  agree on the integration lines, up to an appropriate shift of  $\theta$  by  $\arg Z_s$ .<sup>12</sup>

We want to rewrite the equations in terms of  $x_\gamma^+$  and  $x_\gamma^-$ , the values of the cross-ratios  $X_\gamma$  at the physical values  $\zeta = 1$  and  $\zeta = i$ . This is easy: we set  $\zeta = 1$  and  $\zeta = i$  in (E.2), solve for  $Z_\gamma$  and  $\bar{Z}_\gamma$  and then insert the result back into (E.2). We find

$$\begin{aligned} \ln X_\gamma(\theta) &= \cosh \theta \ln x_\gamma^+ - i \sinh \theta \ln x_\gamma^- + \\ &+ \frac{1}{2\pi i} \sum_{\gamma' \in \Gamma^+} \Omega(\gamma') \langle \gamma, \gamma' \rangle \int_{\ell_{\gamma'}} \frac{d\theta' \sinh 2\theta}{\sinh(\theta' - \theta) \sinh 2\theta'} \log(1 + X_{\gamma'}(\theta')) \end{aligned} \quad (\text{E.3})$$

Notice that the auxiliary parameters  $Z_\gamma$  have disappeared from the equations and we only have the spacetime cross ratios  $x_\gamma^\pm$ . Notice that the kernel of these modified TBA equations is not symmetric in  $\theta$  and  $\theta'$ . It becomes symmetric if we pick a different choice of rapidity variable,  $u = \frac{\cosh 2\theta}{\sinh 2\theta}$ , so that  $-2d\theta' = du' \sinh^2 2\theta'$ . The usefulness of this alternative rapidity variable will become evident momentarily. General TBA equations with a symmetric kernel

$$\ln X_a(u) = L_a(u) + \frac{1}{2\pi} \sum_b \int_{\ell_b} du' K_{ab}(u, u') \log(1 + X_b(u')) \quad (\text{E.4})$$

can be recast as the conditions for a Yang-Yang functional to be extremized

$$\begin{aligned} YY &= \frac{1}{2\pi} \sum_a \int_{\ell_a} du \left( \rho_a(u) \phi_a(u) - Li_2(-e^{L_a(u) - \phi_a(u)}) \right) + \\ &+ \frac{1}{8\pi^2} \sum_{a,b} \int_{\ell_a} du \int_{\ell_b} du' K_{ab}(u, u') \rho_a(u) \rho_b(u') \end{aligned} \quad (\text{E.5})$$

Indeed the variation with respect to  $\rho$  sets

$$\phi_a(u) + \frac{1}{2\pi} \sum_b \int_{\ell_b} du' K_{ab}(u, u') \rho_b(u') = 0 \quad (\text{E.6})$$

while the variation with respect to  $\phi_a$  sets

$$\rho_a(u) = \log \left( 1 + e^{L_a(u) - \phi_a(u)} \right) \quad (\text{E.7})$$

---

<sup>12</sup> The reader should be cautious in extending this relation away from integration lines: the  $Y_s$  functions are usually defined as analytic continuations from the integration lines, while the  $X_s$  are defined by the integral equations for all  $\theta$  and therefore have discontinuities.

If we set  $\log X_a = L_a - \phi_a$  we recover the TBA equations (E.4). We would like to show now that the interesting part of the regularized area (or better, remainder function) of the minimal surface in  $AdS_3$  coincides with the extremum of the Yang-Yang functional for the modified TBA equations. In a sense, this result makes manifest an important property of the area: it should be the extremum of an action functional with fixed boundary conditions given by the choice of physical cross-ratios.

For convenience, let's take  $N$  to be odd, where the polygon has  $2N$  sides. For even  $N$  there are some slight complications, which pop out in various places in the calculation, only to cancel out at the very end in the remainder function. For that reason, it is simpler to just do formal computations for odd  $N$ , and then recover the even  $N$  results by a soft collinear limit. If  $N$  is odd, there is an antisymmetric matrix  $w_{\gamma, \gamma'}$  which roughly speaking inverts  $\langle \gamma, \gamma' \rangle$ .<sup>13</sup> More precisely, it satisfies  $\sum_{\gamma, \gamma'} Z_\gamma w_{\gamma, \gamma'} \langle \gamma', \gamma'' \rangle = Z_{\gamma''}$  and  $\sum_{\gamma', \gamma''} \langle \gamma, \gamma'' \rangle w_{\gamma', \gamma''} \langle \gamma'', \gamma''' \rangle = \langle \gamma, \gamma''' \rangle$ .

The higher conserved charges of the classical integrable system are hidden in the large positive  $\theta$  asymptotic expansion of  $\log X_\gamma \sim \sum_{n=-1}^{\infty} c_{n, \gamma} e^{-n\theta}$ . An alternative set of charges appear at large negative  $\theta$ :  $\log X_\gamma \sim \sum_{n=-1}^{\infty} \tilde{c}_{n, \gamma} e^{n\theta}$ . The contribution to the regularized area denoted as  $A_{periods} + A_{free}$  in [16]<sup>14</sup> can be computed from the conserved charges as  $i \sum_{\gamma, \gamma'} w_{\gamma, \gamma'} c_{-1, \gamma} c_{1, \gamma'}$ . An alternative expression is  $-i \sum_{\gamma, \gamma'} w_{\gamma, \gamma'} \tilde{c}_{-1, \gamma} \tilde{c}_{1, \gamma'}$ . The cleanest formulae usually arise by averaging the two expressions.

From the TBA equations (E.3) we can compute

$$c_{-1, \gamma} = \frac{1}{2} (\ln x_\gamma^+ - i \ln x_\gamma^-) - \frac{1}{2\pi i} \sum_{\gamma' \in \Gamma^+} \Omega(\gamma') \langle \gamma, \gamma' \rangle \int_{\ell_{\gamma'}} \frac{d\theta' e^{\theta'}}{\sinh 2\theta'} \log(1 + X_{\gamma'}(\theta')) \quad (\text{E.8})$$

$$c_{1, \gamma} = \frac{1}{2} (\ln x_\gamma^+ + i \ln x_\gamma^-) - \frac{1}{2\pi i} \sum_{\gamma' \in \Gamma^+} \Omega(\gamma') \langle \gamma, \gamma' \rangle \int_{\ell_{\gamma'}} \frac{d\theta' e^{3\theta'}}{\sinh 2\theta'} \log(1 + X_{\gamma'}(\theta')) \quad (\text{E.9})$$

$$\tilde{c}_{-1, \gamma} = \frac{1}{2} (\ln x_\gamma^+ + i \ln x_\gamma^-) - \frac{1}{2\pi i} \sum_{\gamma' \in \Gamma^+} \Omega(\gamma') \langle \gamma, \gamma' \rangle \int_{\ell_{\gamma'}} \frac{d\theta' e^{-\theta'}}{\sinh 2\theta'} \log(1 + X_{\gamma'}(\theta')) \quad (\text{E.10})$$

$$\tilde{c}_{1, \gamma} = \frac{1}{2} (\ln x_\gamma^+ - i \ln x_\gamma^-) - \frac{1}{2\pi i} \sum_{\gamma' \in \Gamma^+} \Omega(\gamma') \langle \gamma, \gamma' \rangle \int_{\ell_{\gamma'}} \frac{d\theta' e^{-3\theta'}}{\sinh 2\theta'} \log(1 + X_{\gamma'}(\theta')) \quad (\text{E.11})$$

---

<sup>13</sup> In some cases the set of  $\gamma$ 's is an over complete basis, that is why we cannot find a proper inverse. In the kinematic region considered in [16] one can find a proper inverse.

<sup>14</sup> Recall that  $A$  denotes different pieces of the area. The Wilson loop expectation values are then obtained by  $\langle W \rangle \sim e^{-\frac{R^2}{2\pi\alpha'} (\text{Area})} \sim e^{-\frac{\sqrt{\lambda}}{2\pi} (\text{Area})}$ .

The piece of  $A_{periods} + A_{free}$  with no integrals is

$$A_0 = -\frac{1}{2} \sum_{\gamma, \gamma'} w_{\gamma, \gamma'} \ln x_{\gamma}^+ \ln x_{\gamma'}^- \quad (\text{E.12})$$

The piece with one integral, averaged, is

$$A_{temp} = -\frac{1}{2\pi} \sum_{\gamma \in \Gamma^+} \Omega(\gamma) \int_{\ell_{\gamma}} \frac{d\theta \cosh 2\theta}{\sinh 2\theta} (\sinh \theta \ln x_{\gamma}^+ - i \cosh \theta \ln x_{\gamma}^-) \log(1 + X_{\gamma}(\theta)) \quad (\text{E.13})$$

Notice that the term in parenthesis is  $\partial_{\theta} (\cosh \theta \ln x_{\gamma}^+ - i \sinh \theta \ln x_{\gamma}^-)$ . We can use the modified TBA (E.3) to trade it for  $\partial_{\theta} \ln X_{\gamma}(\theta)$  up to terms which we will combine with the other two-integral pieces of  $A_{periods} + A_{free}$ . Then we can write  $\partial_{\theta} \ln X_{\gamma}(\theta) \log(1 + X_{\gamma'}(\theta')) = \partial_{\theta} (-Li_2(-X_{\gamma}))$  and integrate by parts to

$$A_1 = \frac{1}{\pi} \sum_{\gamma \in \Gamma^+} \Omega(\gamma) \int_{\ell_{\gamma}} \frac{d\theta}{\sinh^2 2\theta} Li_2(-X_{\gamma}) \quad (\text{E.14})$$

The remaining term is

$$A_{temp} - A_1 = \frac{1}{4\pi^2 i} \sum_{\gamma, \gamma' \in \Gamma^+} \Omega(\gamma) \Omega(\gamma') \langle \gamma, \gamma' \rangle \int_{\ell_{\gamma'}} \frac{d\theta'}{\sinh 2\theta'} \int_{\ell_{\gamma}} \frac{d\theta}{\sinh 2\theta} \times \\ \times \cosh 2\theta \partial_{\theta} \left( \frac{\sinh 2\theta}{\sinh(\theta' - \theta)} \right) \log(1 + X_{\gamma'}(\theta')) \log(1 + X_{\gamma}(\theta)) \quad (\text{E.15})$$

We can symmetrize the kernel to  $\frac{1}{\sinh(\theta' - \theta)} + \sinh(\theta' - \theta) \cosh 2(\theta + \theta')$ . The second piece cancels out against the remaining two integral terms and we are left with  $A_{periods} + A_{free} = A_0 + A_1 + A_2$ , where

$$A_2 = \frac{1}{4\pi^2 i} \sum_{\gamma, \gamma' \in \Gamma^+} \Omega(\gamma) \Omega(\gamma') \langle \gamma, \gamma' \rangle \int_{\ell_{\gamma'}} \frac{d\theta'}{\sinh 2\theta'} \int_{\ell_{\gamma}} \frac{d\theta}{\sinh 2\theta} \frac{1}{\sinh(\theta' - \theta)} \\ \log(1 + X_{\gamma'}(\theta')) \log(1 + X_{\gamma}(\theta)) \quad (\text{E.16})$$

We see that  $A_{periods} + A_{free} = A_0 + YY_{cr}$ , where  $YY_{cr}$  is the critical value of the  $YY$  functional. In summary, the full area of the surface can be written as  $A = A_{div} + A_{BDS-like} + A_0 + YY_{cr}$ , where  $YY_{cr} = A_1 + A_2$  in (E.14) and (E.16).  $A_{div}$  are the divergent terms and  $A_{BDS-like}$  can be found in formula (5.10) in [25]. We see that  $YY_{cr}$  is manifestly small in the region where the  $X_{\gamma}$  are small, which is when the  $x_{\gamma}^{\pm}$  are small. We also expect that  $A_{BDS-like} - A_{BDS} + A_0$  becomes small in this region. This is an expression written purely in terms of the spacetime cross ratios.

*E.1. Evaluating the OPE for general configurations in AdS<sub>3</sub>*

In this subsection we expand the OPE with AdS<sub>3</sub> kinematics in the case that we split the polygon into two general subpolygons.

If we are given any functional  $F[x]$  and a small deformation  $F[x] + f[x, y]$ , we can ask what is the relation between the critical values  $F_{cr}$  and  $(F + f)_{cr}$ . It is elementary to show that the difference of the two critical values can be computed as the critical value of  $f[x_{cr}, y]$ , where  $x_{cr}$  extremizes  $F(x)$ . We can immediately apply this to the case of the Yang-Yang functionals. We take  $F = YY[c]$ , the Yang-Yang functional with a certain label  $c \in \Gamma^+$  erased, and  $f$  is the remaining part (notice that kernel  $K_{cc}$  is always zero for us)

$$f = \frac{1}{2\pi} \int_{\ell_c} du \left( \rho_c(u) \phi_c(u) - Li_2(-e^{L_c(u) - \phi_c(u)}) \right) + \frac{1}{4\pi^2} \sum_b \int_{\ell_c} du \int_{\ell_b} du' K_{cb}(u, u') \rho_c(u) \rho_b(u') \quad (\text{E.17})$$

The extremum of  $f$  with respect to  $\rho_c$  and  $\phi_c$  is simply

$$f_{cr} = YY_{cr} - YY[c]_{cr} \sim -\frac{1}{2\pi} \int_{\ell_c} du Li_2(-X_c(u)) \sim \frac{1}{2\pi} \int_{\ell_c} du X_c(u) \quad (\text{E.18})$$

where

$$\ln X_c(u) = L_c(u) + \frac{1}{2\pi} \sum_b \int_{\ell_b} du' K_{cb}(u, u') \log(1 + X_b(u')) \quad (\text{E.19})$$

The soft limit OPE we consider in this paper leads exactly to this sort of decoupling limits. For simplicity, we can consider the simple kinematic region of [16]. In the AdS<sub>3</sub> case, if we decompose a  $2N$ -gon into a  $2n + 2$ -gon and  $2N - 2n + 2$ -gon by applying the  $\tau$  rescaling to the  $x^+$  coordinates, it is easy to see that  $Z_{n-1}$  acquires a large real part, so that  $x_{n-1}^+$  becomes very small, scaling as  $e^{-\tau}$ , while all the other  $x_\gamma^+$  and  $x_\gamma^-$  are held fixed. Indeed,  $YY[n-1]$  is the sum of the Yang-Yang functionals for the  $2n + 2$ -gon and  $2N - 2n + 2$ -gon. Then the leading exponential behavior is controlled by

$$f_{cr} = YY_{cr} - YY[n-1]_{cr} \sim \frac{1}{2\pi} \int_{\ell_{n-1}} du e^{\ln x_{n-1}^+ \cosh \theta - i \ln x_{n-1}^- \sinh \theta} C_1(\theta) C_2(\theta) \quad (\text{E.20})$$

where

$$\ln C_1(\theta) = \frac{1}{2\pi} \sum_{s < n-1} \int_{\ell_b} du' K_{cb}(u, u') \log(1 + X_b(u')) \quad (\text{E.21})$$

and

$$\ln C_2(\theta) = \frac{1}{2\pi} \sum_{s > n-1} \int_{\ell_b} du' K_{cb}(u, u') \log(1 + X_b(u')) \quad (\text{E.22})$$

are interpreted naturally as the density of one-particle excitations on the GKP string [7] created by the  $2n + 2$ -gon and  $2N - 2n + 2$ -gon respectively.

## Appendix F. The modified TBA and Yang-Yang functional for $AdS_5$ null polygons

In this section we generalize the results of the previous section to the most general  $AdS_5$  kinematics. For convenience, we take the number of gluons  $n$  to be odd. The case where  $n$  is even can be recovered by a soft collinear limit. In the notations of [16] the TBA equations take the form

$$\begin{aligned}\log Y_{2,s}(\theta) &= -|m_s| \sqrt{2} \cosh(\theta - i\phi_s) - K_2 \star \alpha_s - K_1 \star \beta_s \\ \log Y_{1,s}(\theta) &= -|m_s| \cosh(\theta - i\phi_s) - C_s - \frac{1}{2} K_2 \star \beta_s - K_1 \star \alpha_s - \frac{1}{2} K_3 \star \gamma_s \\ \log Y_{3,s}(\theta) &= -|m_s| \cosh(\theta - i\phi_s) + C_s - \frac{1}{2} K_2 \star \beta_s - K_1 \star \alpha_s + \frac{1}{2} K_3 \star \gamma_s\end{aligned}\quad (\text{F.1})$$

where  $\star$  denotes convolution. The kernels are

$$K_1(\theta) = \frac{1}{2\pi \cosh \theta}, \quad K_2(\theta) = \frac{\sqrt{2} \cosh \theta}{\pi \cosh 2\theta}, \quad K_3(\theta) = \frac{i}{\pi} \tanh 2\theta \quad (\text{F.2})$$

and

$$\begin{aligned}\alpha_s &\equiv \log \frac{(1 + Y_{1,s})(1 + Y_{3,s})}{(1 + Y_{2,s-1})(1 + Y_{2,s+1})}, \quad \gamma_s \equiv \log \frac{(1 + Y_{1,s-1})(1 + Y_{3,s+1})}{(1 + Y_{1,s+1})(1 + Y_{3,s-1})}, \\ \beta_s &\equiv \log \frac{(1 + Y_{2,s})^2}{(1 + Y_{1,s-1})(1 + Y_{1,s+1})(1 + Y_{3,s-1})(1 + Y_{3,s+1})}.\end{aligned}\quad (\text{F.3})$$

We now have three parameters per column  $s$ : the magnitude of the *mass*  $|m_s|$ , its phase  $\phi_s$  and the *chemical potential*  $C_s$ . As explained in the  $AdS_3$  case we can eliminate them in favor of physical cross-ratios  $y_{a,s} \equiv \widehat{Y}_{a,s}(0)$  where  $a = 1, 2, 3$ . The hatted  $Y$ -functions are defined in the appendix D of [16] and are given by  $\widehat{Y}_{a,s}(\theta) = Y_{a,s}(\theta)$  if  $a + s$  is even and  $\widehat{Y}_{a,s}(\theta) = Y_{a,s}(\theta - i\pi/4)$  for  $a + s$  odd. The modified TBA equations then read

$$\begin{aligned}\log \widehat{Y}_{2,s} - E_s &= -\widetilde{K}_2 \diamond \widehat{\alpha}_s - \widetilde{K}_1 \diamond \widehat{\beta}_s, \\ \log \widehat{Y}_{1,s} \widehat{Y}_{3,s} - \sqrt{2} E_s^{[(-)^{s+1}]} &= -\widetilde{K}_2^{[2(-)^{s+1}]} \diamond \widehat{\beta}_s - 2\widetilde{K}_1 \diamond \widehat{\alpha}_s, \\ \log \widehat{Y}_{1,s} / \widehat{Y}_{3,s} - \log y_{1,s} / y_{3,s} &= -\widetilde{K}_3 \diamond \widehat{\gamma}_s,\end{aligned}\quad (\text{F.4})$$

where  $f^{[m]}(\theta, \theta') = f(\theta + im\pi/4, \theta')$ ,  $\{\widehat{\alpha}_s, \widehat{\beta}_s, \widehat{\gamma}_s\}$  are  $\{\alpha_s, \beta_s, \gamma_s\}$  evaluated on the hatted  $Y$ 's and  $E_s = -i(-1)^s (\sqrt{2} \sinh[\theta + (-)^s i\pi/4] \log y_{2,s} - \sinh[\theta] \log y_{1,s} y_{3,s})$  is the new source which depends only on the physical cross ratios. The modified kernels read

$$\widetilde{K}_1 = -\frac{1}{2\pi} \frac{\sinh(2\theta)}{\sinh(2\theta') \cosh(\theta - \theta')} \quad \widetilde{K}_3 = \frac{i}{\pi} \frac{\sinh(2\theta)}{\sinh(2\theta - 2\theta') \sinh(2\theta')} \quad (\text{F.5})$$



and

$$K_2 = i\sqrt{2} \sinh[\theta - \theta' + (-)^s i\pi/4] \tilde{K}_3. \quad (\text{F.6})$$

Notice that in (F.4),  $\diamond$  no longer denotes a convolution but instead an application of an integral kernel  $\tilde{K}(\theta, \theta')$ . Let us denote the right hand side of the three equations in (F.4) by  $\hat{\mathcal{A}}_{2,s}$ ,  $\hat{\mathcal{A}}_{1,s} + \hat{\mathcal{A}}_{3,s}$  and  $\hat{\mathcal{A}}_{1,s} - \hat{\mathcal{A}}_{3,s}$  respectively. The contribution  $A_{periods} + A_{extra}$  can then be computed as explained in the previous sections. The result turns out to be simply given by

$$A_{periods} + A_{extra} = A_0 + YY_c, \quad (\text{F.7})$$

where

$$YY_c = \sum_{a,s} \int \frac{d\theta}{\pi \sinh^2(2\theta)} \left[ Li_2(-\hat{Y}_{a,s}) - \frac{1}{2} \log(1 + \hat{Y}_{a,s}) \hat{\mathcal{A}}_{a,s} \right] \quad (\text{F.8})$$

is the value of the Yang-Yang functional at the extremum. Note that the natural particle rapidities are again given by  $u$ .

The piece  $A_0$  is very much like  $A_{periods}$  and is given by  $A_0 = -\frac{i}{2} \bar{v}_{a,s} \omega_{a,s;a's'} v_{a's'}$  where

$$v_{a,s} = \frac{i}{4} \left[ 2 \log y_{2,s} - (1 + i(-1)^{s+1}) \log y_{1,s} y_{3,s} \right] (-1)^{s+1} (1 - (-1)^{s+1} i)^{\delta_{a,2}}, \quad (\text{F.9})$$

$\bar{v}_{a,s}$  is the complex conjugate vector, and  $\omega_{a,s;a's'}$  is the inverse of the intersection form of cycles and is given in [16].

### F.1. Explicit details for the hexagon

In order to illustrate how the kernels of the modified TBA and the Yang-Yang functional emerge in a concrete, relatively simple example, we can consider the case of the hexagon in full, tedious detail. We are interested in a limit where one of the three cross-ratios, conventionally  $u_2$ , goes to zero, while the other two remain finite, and their sum  $u_1 + u_3$  approaches 1. At strong coupling, this conditions constrain the behavior of the conserved spin four current  $P(z)$ : the two zeroes of the polynomial  $P(z)$  are far from each other in a specific direction. In the language of [15] this limit corresponds to a large absolute value of the “period”  $Z$  with phase  $\varphi \sim -\pi/4$ ,  $\hat{\varphi} = \varphi + \pi/4 \sim 0$  (more precisely, we will take it to be slightly positive).

Compared to the previous section, we now have only one value of  $s$  and only three  $Y$  functions  $Y_a = Y_{1,a}$ . One of the three TBA equations is trivially solved, since the ratio

$Y_1/Y_3$  is constant. The other two equations for  $\log Y_2$  and  $\log Y_1 Y_3$  reduce to the equations in [15] (see (3.6) and (3.7) in [15])

$$\epsilon(\theta - i\hat{\varphi}) = Ze^{i\pi/4-\theta} + \bar{Z}e^{\theta-i\pi/4} + \int d\theta' K_2(\theta - \theta') \tilde{L}(\theta') + \int d\theta' K_1(\theta - \theta') L(\theta') \quad (\text{F.10})$$

$$\tilde{\epsilon}(\theta - i\hat{\varphi}) = \sqrt{2}(Ze^{i\pi/4-\theta} + \bar{Z}e^{\theta-i\pi/4}) + \int d\theta' 2K_1(\theta - \theta') \tilde{L}(\theta') + \int d\theta' K_2(\theta - \theta') L(\theta') \quad (\text{F.11})$$

We denote as  $\tilde{L}(\theta) = \log(1 + e^{-\tilde{\epsilon}(\theta - i\hat{\varphi})})$  and  $L(\theta) = \log(1 + \mu e^{-\epsilon(\theta - i\hat{\varphi})})(1 + \mu^{-1} e^{-\epsilon(\theta - i\hat{\varphi})})$ . We shifted the integration variables for convenience. Remember the correct integration paths: the real part of  $\theta'$  runs from  $-\infty$  to  $\infty$ , the imaginary part is fixed at  $\hat{\varphi}$ .

We can evaluate the equations at  $\theta = 0$  and  $i\pi/4$  in order to trade  $Z$  for cross-ratios.

$$Z + \bar{Z} = \log(b_1) - \int d\theta' K_2(\theta' - i\pi/4) \tilde{L}(\theta') - \int d\theta' K_1(\theta' - i\pi/4) L(\theta') \quad (\text{F.12})$$

and

$$\sqrt{2}(Ze^{i\pi/4} + \bar{Z}e^{-i\pi/4}) = \log(1/u_2 - 1) - \int d\theta' 2K_1(\theta') \tilde{L}(\theta') - \int d\theta' K_2(\theta') L(\theta') \quad (\text{F.13})$$

We need to decompose

$$Ze^{i\pi/4-\theta} + \bar{Z}e^{\theta-i\pi/4} = -i(Z + \bar{Z})\sqrt{2} \sinh(\theta) + i(Ze^{i\pi/4} + \bar{Z}e^{-i\pi/4})\sqrt{2} \sinh(\theta - i\pi/4) \quad (\text{F.14})$$

so that we are ready to substitute

$$Ze^{i\pi/4-\theta} + \bar{Z}e^{\theta-i\pi/4} = E(\theta) - \frac{\sqrt{2}}{\pi} \int d\theta' \frac{\sinh(\theta + \theta')}{\sinh 2\theta'} \tilde{L}(\theta') - \frac{1}{\pi} \int d\theta' \frac{\cosh(\theta' + \theta)}{\cosh 2\theta'} L(\theta') \quad (\text{F.15})$$

in the TBA equations. Here we define

$$E(\theta) = -i\sqrt{2} \sinh \theta \log(b_1) + i \sinh(\theta - i\pi/4) \log(1/u_2 - 1). \quad (\text{F.16})$$

We get the new kernels

$$\begin{aligned} \epsilon(\theta - i\hat{\varphi}) = E(\theta) &- \frac{\sqrt{2}}{\pi} \int d\theta' \frac{\cosh 2\theta \sinh(\theta - \theta')}{\cosh 2(\theta - \theta') \sinh 2\theta'} \tilde{L}(\theta') \\ &- \frac{1}{2\pi} \int d\theta' \frac{\cosh 2\theta}{\cosh(\theta - \theta') \cosh 2\theta'} L(\theta') \end{aligned} \quad (\text{F.17})$$

and

$$\begin{aligned}\tilde{\epsilon}(\theta - i\hat{\varphi}) &= \sqrt{2}E(\theta) - \frac{1}{\pi} \int d\theta' \frac{\sinh 2\theta}{\cosh(\theta - \theta') \sinh 2\theta'} \tilde{L}(\theta') \\ &\quad - \frac{\sqrt{2}}{\pi} \int d\theta' \frac{\sinh 2\theta \sinh(\theta - \theta')}{\cosh 2(\theta - \theta') \cosh 2\theta'} L(\theta')\end{aligned}\tag{F.18}$$

In order to compute  $A_{periods} + A_{free}$  it is useful to go back to the original expression for the regularized area, involving the conserved quantities hidden in the large  $\theta$  asymptotic expansion of the  $\epsilon$  and  $\tilde{\epsilon}$  functions. If we denote the coefficients of the expansion as

$$\epsilon(\theta) \sim \sum_{n=-1}^{\infty} \epsilon_n e^{-n\theta} \quad \tilde{\epsilon}(\theta) \sim \sum_{n=-1}^{\infty} \tilde{\epsilon}_n e^{-n\theta},\tag{F.19}$$

then

$$A_{periods} + A_{free} = -\frac{i}{2} \left( e^{i\pi/4} \epsilon_{-1} \tilde{\epsilon}_1 - e^{-i\pi/4} \tilde{\epsilon}_{-1} \epsilon_1 \right).\tag{F.20}$$

We can expand in powers of  $e^{-\theta}$

$$\begin{aligned}\epsilon(\theta - i\hat{\varphi}) &\sim E(\theta) - \frac{\sqrt{2}}{\pi} \int d\theta' \left( \frac{1}{4} \left( \frac{1}{\sinh \theta'} + \frac{1}{\cosh \theta'} \right) e^\theta - \frac{e^{3\theta'}}{2 \sinh 2\theta'} e^{-\theta} \right) \tilde{L}(\theta') \\ &\quad - \frac{1}{2\pi} \int d\theta' \left( \frac{e^{\theta+\theta'}}{\cosh 2\theta'} - \frac{e^{3\theta'}}{\cosh 2\theta'} e^{-\theta} \right) L(\theta')\end{aligned}\tag{F.21}$$

$$\begin{aligned}\tilde{\epsilon}(\theta - i\hat{\varphi}) &\sim \sqrt{2}E(\theta) - \frac{1}{\pi} \int d\theta' \left( \frac{1}{2} \left( \frac{1}{\sinh \theta'} + \frac{1}{\cosh \theta'} \right) e^\theta - \frac{e^{3\theta'}}{\sinh 2\theta'} e^{-\theta} \right) \tilde{L}(\theta') \\ &\quad - \frac{\sqrt{2}}{\pi} \int d\theta' \frac{1}{2} \left( \frac{e^{\theta+\theta'}}{\cosh 2\theta'} - \frac{e^{3\theta'}}{\cosh 2\theta'} e^{-\theta} \right) L(\theta')\end{aligned}\tag{F.22}$$

Notice that at the order which matters, the expansions of  $\epsilon$  and  $\tilde{\epsilon}$  are simply proportional:  $\tilde{\epsilon}_{-1} \sim \sqrt{2}\epsilon_{-1}$  and  $\tilde{\epsilon}_1 \sim \sqrt{2}\epsilon_1$ . The proportionality implies that  $A_{periods} + A_{free} = \frac{i}{2}\epsilon_{-1}\epsilon_1\sqrt{2}(e^{i\pi/4} - e^{-i\pi/4}) = -\epsilon_{-1}\epsilon_1$ . We can read off the relevant pieces of the expansion

$$\epsilon_{-1} = E_{-1} - \frac{1}{\sqrt{2}\pi} \int d\theta' \frac{e^{\theta'}}{\sinh 2\theta'} \tilde{L}(\theta') - \frac{1}{2\pi} \int d\theta' \frac{e^{\theta'}}{\cosh 2\theta'} L(\theta')\tag{F.23}$$

$$\epsilon_1 = E_1 + \frac{1}{\sqrt{2}\pi} \int d\theta' \frac{e^{3\theta'}}{\sinh 2\theta'} \tilde{L}(\theta') + \frac{1}{2\pi} \int d\theta' \frac{e^{3\theta'}}{\cosh 2\theta'} L(\theta')\tag{F.24}$$

where

$$E_{-1} = -\frac{i}{\sqrt{2}} \log(b_1) + \frac{i}{2} e^{-i\pi/4} \log(1/u_2 - 1)\tag{F.25}$$

and

$$E_1 = \frac{i}{\sqrt{2}} \log(b_1) - \frac{i}{2} e^{i\pi/4} \log(1/u_2 - 1) \quad (\text{F.26})$$

Actually, the most useful expression for  $A_{periods} + A_{free}$  is the average of the expression derived from the large  $\theta$  asymptotics and the expression derived from the small  $\theta$  asymptotics. Setting  $\epsilon \sim \epsilon'_1 e^{-\theta} + \epsilon'_{-1} e^{\theta} + \dots$  and a similar expression for  $\tilde{\epsilon}$ , which again equals  $\sqrt{2}\epsilon$  at this expansion order,

$$\epsilon'_{-1} \sim E_{-1} - \frac{1}{\sqrt{2}\pi} \int d\theta' \frac{e^{-3\theta'}}{\sinh 2\theta'} \tilde{L}(\theta') + \frac{1}{2\pi} \int d\theta' \frac{e^{-3\theta'}}{\cosh 2\theta'} L(\theta') \quad (\text{F.27})$$

$$\epsilon'_1 \sim E_1 + \frac{1}{\sqrt{2}\pi} \int d\theta' \frac{e^{-\theta'}}{\sinh 2\theta'} \tilde{L}(\theta') - \frac{1}{2\pi} \int d\theta' \frac{e^{-\theta'}}{\cosh 2\theta'} L(\theta') \quad (\text{F.28})$$

Putting all together, we can organize the final result in terms with two, one or zero contour integrals:  $\epsilon_1 \epsilon_{-1} = A_2 + A_1 + A_0$ .

$$A_0 = (-i/\sqrt{2} \log(b_1) + i/2 e^{-i\pi/4} \log(1/u_2 - 1))(i/\sqrt{2} \log(b_1) - i/2 e^{i\pi/4} \log(1/u_2 - 1)) \quad (\text{F.29})$$

simplifies to

$$A_0 = \frac{1}{4} \log^2 b_1 + \frac{1}{4} \log^2(b_3 - 1/b_1) \quad (\text{F.30})$$

In the next term, we can average the two available expressions and split again  $A_1 = A_{1,1} + A_{1,2}$

$$A_{1,1} = \frac{1}{\sqrt{2}\pi} \int d\theta' \left( -i\sqrt{2} \log(b_1) \cosh \theta' + i \log(1/u_2 - 1) \right) \cosh(\theta' - i\pi/4) \frac{\cosh 2\theta'}{\sinh 2\theta'} \tilde{L}(\theta') \quad (\text{F.31})$$

$$A_{1,2} = \frac{1}{2\pi} \int d\theta' \left( -i\sqrt{2} \log(b_1) \cosh \theta' + i \log(1/u_2 - 1) \right) \cosh(\theta' - i\pi/4) \frac{\sinh 2\theta'}{\cosh 2\theta'} L(\theta') \quad (\text{F.32})$$

Next we would like to replace the term in parenthesis with the  $\theta$  derivatives of  $\tilde{\epsilon}$  and  $\epsilon$  respectively, to allow for a useful integration by parts. The difference between the terms in parenthesis and the  $\theta$  derivatives will generate new terms to be added to  $A_2$ :  $A_{1,1} = A'_{1,1} + A_{2,1} + A_{2,2}$  and  $A_{1,2} = A'_{1,2} + A_{2,3} + A_{2,4}$ .

$$A'_{1,1} = \frac{1}{2\pi} \int d\theta' \partial_{\theta'} \tilde{\epsilon}(\theta' - i\hat{\varphi}) \frac{\cosh 2\theta'}{\sinh 2\theta'} \tilde{L}(\theta') \quad (\text{F.33})$$

$$A'_{1,2} = \frac{1}{2\pi} \int d\theta' \partial_{\theta'} \epsilon(\theta' - i\hat{\varphi}) \frac{\sinh 2\theta'}{\cosh 2\theta'} L(\theta') \quad (\text{F.34})$$

$$A_{2,1} = \frac{1}{\sqrt{2\pi}} \int d\theta \frac{1}{\sqrt{2\pi}} \int d\theta' \partial_\theta \left( \frac{\sinh 2\theta}{\cosh(\theta - \theta') \sinh 2\theta'} \right) \tilde{L}(\theta') \frac{\cosh 2\theta}{\sinh 2\theta} \tilde{L}(\theta) \quad (\text{F.35})$$

$$A_{2,2} = \frac{1}{\sqrt{2\pi}} \int d\theta \frac{1}{\pi} \int d\theta' \partial_\theta \left( \frac{\sinh 2\theta \sinh(\theta - \theta')}{\cosh 2(\theta - \theta') \cosh 2\theta'} \right) L(\theta') \frac{\cosh 2\theta}{\sinh 2\theta} \tilde{L}(\theta) \quad (\text{F.36})$$

$$A_{2,3} = \frac{1}{2\pi} \int d\theta \frac{\sqrt{2}}{\pi} \int d\theta' \partial_\theta \left( \frac{\cosh 2\theta \sinh(\theta - \theta')}{\cosh 2(\theta - \theta') \sinh 2\theta'} \right) \tilde{L}(\theta') \frac{\sinh 2\theta}{\cosh 2\theta} L(\theta) \quad (\text{F.37})$$

$$A_{2,4} = \frac{1}{2\pi} \int d\theta \frac{1}{2\pi} \int d\theta' \partial_\theta \left( \frac{\cosh 2\theta}{\cosh(\theta - \theta') \cosh 2\theta'} \right) L(\theta') \frac{\sinh 2\theta}{\cosh 2\theta} L(\theta) \quad (\text{F.38})$$

On the other hand, we can decompose  $A_2 = A_{2,5} + A_{2,6} + A_{2,7}$ , averaging the two expressions and symmetrizing

$$A_{2,5} = -\frac{1}{\sqrt{2\pi}} \int d\theta \frac{1}{\sqrt{2\pi}} \int d\theta' \frac{\cosh 2(\theta + \theta') \cosh(\theta - \theta')}{\sinh 2\theta \sinh 2\theta'} \tilde{L}(\theta') \tilde{L}(\theta) \quad (\text{F.39})$$

$$A_{2,6} = -\frac{\sqrt{2}}{\pi} \int d\theta \frac{1}{2\pi} \int d\theta' \frac{\sinh 2(\theta + \theta') \cosh(\theta - \theta')}{\cosh 2\theta' \sinh 2\theta} L(\theta') \tilde{L}(\theta) \quad (\text{F.40})$$

$$A_{2,7} = -\frac{1}{2\pi} \int d\theta \frac{1}{2\pi} \int d\theta' \frac{\cosh 2(\theta + \theta') \cosh(\theta - \theta')}{\cosh 2\theta \cosh 2\theta'} L(\theta') L(\theta) \quad (\text{F.41})$$

Combining pieces together vast simplifications occur

$$A_{2,1} + A_{2,5} = \frac{1}{\sqrt{2\pi}} \int d\theta \frac{1}{\sqrt{2\pi}} \int d\theta' \frac{1}{\sinh 2\theta \sinh 2\theta' \cosh(\theta - \theta')} \tilde{L}(\theta') \tilde{L}(\theta) \quad (\text{F.42})$$

$$A_{2,2} + A_{2,3} + A_{2,6} = \frac{\sqrt{2}}{\pi} \int d\theta \frac{1}{\pi} \int d\theta' \frac{\sinh(\theta - \theta')}{\cosh 2\theta' \sinh 2\theta \cosh(2\theta - 2\theta')} L(\theta') \tilde{L}(\theta) \quad (\text{F.43})$$

$$A_{2,4} + A_{2,7} = -\frac{1}{2\pi} \int d\theta \frac{1}{2\pi} \int d\theta' \frac{1}{\cosh 2\theta \cosh 2\theta' \cosh(\theta - \theta')} L(\theta') L(\theta) \quad (\text{F.44})$$

On the other hand, the pieces to be integrated by parts give

$$A'_{1,1} = \frac{1}{\pi} \int d\theta' \frac{1}{\sinh^2 2\theta'} Li_2(-e^{-\tilde{\epsilon}(\theta' - i\hat{\varphi})}) \quad (\text{F.45})$$

$$A'_{1,2} = -\frac{1}{\pi} \int d\theta' \frac{1}{\cosh^2 2\theta'} \left( Li_2(-\mu e^{-\epsilon(\theta' - i\hat{\varphi})}) + Li_2(-\mu^{-1} e^{-\epsilon(\theta' - i\hat{\varphi})}) \right) \quad (\text{F.46})$$

Here  $Li_2$  indicates Mathematica *PolyLog*[2,  $x$ ].

In summary, the final result for  $A_{periods} + A_{free}$  is given by (F.30) plus the critical value of the Yang-Yang functional which is the sum of (F.42)-(F.46). This is the Yang-Yang functional for the integral equations in (F.17)(F.18), written in terms of the new variable  $du = -\frac{2d\theta}{\sinh^2 2\theta}$  which makes the kernels symmetric. A shift in the integration contour in (F.46) takes it to the form in (F.8).

### F.2. Easy pieces of the hexagon

Here we focus on the terms of the strong coupling answer for the hexagon which contain no integrals. In particular we focus on such terms for the remainder function. These terms come from (F.30) plus  $A_{BDS-like} - A_{BDS}$ , given in [15]. This gives<sup>15</sup>

$$R_{easy} = -\frac{1}{4} (\log^2 b_1 + \log^2(b_3 - 1/b_1)) + \frac{1}{8} \sum_i (\log^2 u_i + 2Li_2(1 - u_i)) \quad (F.47)$$

we have  $u_1 = \frac{1}{b_2 b_3}$ ,  $u_2 = \frac{1}{b_1 b_3}$ ,  $u_3 = \frac{1}{b_1 b_2}$ . We can write everything in terms of  $b_1, b_3$  and  $\mu = -2 \cos \phi$  by using  $b_2 = \frac{b_1 + b_3 - 2 \cos \phi}{b_1 b_3 - 1}$ . The limit we are interested in is then  $b_1$  and  $b_3$  of the same order and very large with  $\phi$  fixed. One can explicitly check that the above combination is finite in such limit. One question we would like to answer is whether we could get problematic terms of the form  $u_2^p \log^q u_2$  in the small  $u_2$  expansion. Such terms could only come from the following piece in the above answer (remember that  $u_1 + u_3 = 1$  in the limit.):

$$R_{easy-part} = -\frac{1}{4} (\log^2 b_1 + \log^2(b_3 - 1/b_1)) + \frac{1}{8} (\log^2 u_2 + 2Li_2(1 - u_2)) \quad (F.48)$$

Note that this can be entirely written in terms of  $b_1$  and  $b_3$ . In order to show that this does not contain the kind of terms mentioned above we use:  $Li_2(1 - u_2) = -Li_2(u_2) - \log u_2 \log(1 - u_2) + \frac{\pi^2}{6}$ . Furthermore, we call  $z^2 = \frac{b_1}{b_3}$ , then we obtain

$$R_{easy-part} = \frac{\pi^2}{24} - \frac{1}{4} (\log^2(1 - u_2) - 2 \log(1 - u_2) \log z + 2 \log^2 z - Li_2 u_2) \quad (F.49)$$

From this is clear that in the small  $u_2$  expansion we will not get problematic terms, just simple power series. Furthermore, in this form it is very easy to expand.

### F.3. Expanding the hexagon at strong coupling

We choose the following six points,  $P = (Z_{-1}, Z_0, Z_1, Z_2, Z_3, Z_4)$ , as

$$\begin{aligned} P_1 &= (1, e^{-2\tau}, e^{-2\tau}, 1, 0, 0), & P_3 &= (e^{-2\tau}, 1, -1, -e^{-2\tau}, 0, 0), \\ P_2 &= (\sinh(\tau + \sigma), \sinh(\tau - \sigma), -\cosh(\tau - \sigma), \cosh(\tau + \sigma), -i\sqrt{2} \cos \phi, i\sqrt{2} \sin \phi) \\ P_6 &= (1, 1, 1, 1, 0, 0), & P_4 &= (1, 1, -1, -1, 0, 0), & P_5 &= (0, 0, 1, -1, i\sqrt{2}, 0) \end{aligned} \quad (F.50)$$

---

<sup>15</sup> Recall the relative sign between the remainder function and the area  $R \sim \log W \propto -\text{Area}$ . We are ignoring a factor of  $\sqrt{\lambda}/(2\pi)$ .

We then define  $u_i = \frac{d_{i+1,i+5}^2 d_{i+2,i+4}^2}{d_{i+1,i+4}^2 d_{i+2,i+5}^2}$ . We obtain (4.1). We also define  $b_i = \sqrt{\frac{u_i}{u_{i+1} u_{i+2}}}$ . These are

$$b_2 = 2(\cosh \tau \cosh \sigma - \cos \phi) / \sinh^2 \tau, \quad b_1 = e^\sigma \cosh \tau, \quad b_3 = e^{-\sigma} \cosh \tau \quad (\text{F.51})$$

This implies that  $\mu$  defined via  $\mu + \mu^{-1} = b_1 b_2 b_3 - b_1 - b_2 - b_3 = -2 \cos \phi$ , is  $\mu = -e^{i\phi}$ .

The remainder function is  $R = -\frac{\sqrt{\lambda}}{2\pi}(\text{Area})$ . We will suppress the factor of  $\frac{\sqrt{\lambda}}{2\pi}$  but we will take into account the minus sign. Let us now expand the various terms to the desired order. Inserting (F.51) and (4.1) into (F.47) and expanding we get

$$\begin{aligned} R_{\text{easy}} &\sim -\cos \phi e^{-\tilde{\tau}} [\cosh \sigma \log[2 \cosh \sigma] - \sigma \sinh \sigma] + \\ &\quad + e^{-2\tilde{\tau}} \left[ \frac{\log[2 \cosh \sigma] - \sigma}{2} + \cos 2\phi g(\sigma) \right] \\ g(\sigma) &= -\frac{1}{4} \cosh 2\sigma \log[2 \cosh \sigma] + \frac{1}{4} \sigma \sinh 2\sigma + \frac{1}{8} \end{aligned} \quad (\text{F.52})$$

where  $e^{-\tilde{\tau}} = e^{-\tau}/2$ . There is a constant term that we neglected. Note that individual terms in (F.47) diverge, but the combination is finite, which is what we expected for the remainder function.

The leading order expansion of the Yang-Yang functional comes only from the di-logarithm piece. Expanding the di-logarithm in (F.45) (F.46) to first order we get

$$\begin{aligned} R_{YY} = -YY_{cr} &\sim \frac{1}{\pi} \int d\theta \left[ \frac{1}{\sinh^2 2\theta} e^{-\sqrt{2}E(\theta)} - \frac{(\mu + \mu^{-1})}{\cosh^2 2\theta} e^{-E(\theta)} \right] \\ E(\theta) &= \sqrt{2}[\tilde{\tau} \cosh \theta - i\sigma \sinh \theta] \end{aligned} \quad (\text{F.53})$$

We first used the leading order expressions for  $\epsilon(\theta - i\hat{\phi})$  in (F.17),(F.18), to get the first line. The second line is the approximate expression for (F.16) using the leading order expressions for the cross ratios

$$\begin{aligned} -\log y_2 &= \log\left[\frac{1}{u_2} - 1\right] \sim -\log u_2 \sim -2\tilde{\tau} \\ \log b_1 &= -\frac{1}{2} \log y_1 y_3 \sim \tilde{\tau} + \sigma \end{aligned} \quad (\text{F.54})$$

Of course, in deriving (F.52) it was important to go beyond this leading order expression. (F.52) and (F.53) are the expansions quoted in the main text (4.2), up to the trivial relabeling  $\tilde{\tau} \rightarrow \tau$ .

## References

- [1] A. A. Belavin, A. M. Polyakov and A. B. Zamolodchikov, Nucl. Phys. B **241**, 333 (1984).
- [2] L. F. Alday and J. M. Maldacena, JHEP **0706**, 064 (2007) [arXiv:0705.0303 [hep-th]].
- [3] J. M. Drummond, G. P. Korchemsky and E. Sokatchev, Nucl. Phys. B **795**, 385 (2008) [arXiv:ward [hep-th]].
- [4] A. Brandhuber, P. Heslop and G. Travaglini, Nucl. Phys. B **794**, 231 (2008) [arXiv:0707.1153 [hep-th]].
- [5] J. M. Drummond, J. Henn, G. P. Korchemsky and E. Sokatchev, Nucl. Phys. B **815**, 142 (2009) [arXiv:0803.1466 [hep-th]].
- [6] Z. Bern, L. J. Dixon, D. A. Kosower, R. Roiban, M. Spradlin, C. Vergu and A. Volovich, Phys. Rev. D **78**, 045007 (2008) [arXiv:0803.1465 [hep-th]].
- [7] S. S. Gubser, I. R. Klebanov and A. M. Polyakov, Nucl. Phys. B **636**, 99 (2002) [arXiv:hep-th/0204051].
- [8] N. Beisert, B. Eden and M. Staudacher, J. Stat. Mech. **0701**, P021 (2007) [arXiv:hep-th/0610251].
- [9] B. Basso, to appear.
- [10] Z. Bern, L. J. Dixon and V. A. Smirnov, Phys. Rev. D **72**, 085001 (2005) [arXiv:hep-th/0505205].
- [11] J. M. Drummond, J. Henn, G. P. Korchemsky and E. Sokatchev, Nucl. Phys. B **826**, 337 (2010) [arXiv:0712.1223 [hep-th]].
- [12] L. F. Alday and J. Maldacena, JHEP **0711**, 068 (2007) [arXiv:0710.1060 [hep-th]].
- [13] J. M. Drummond, J. Henn, G. P. Korchemsky and E. Sokatchev, Phys. Lett. B **662**, 456 (2008) [arXiv:0712.4138 [hep-th]].
- [14] C. Anastasiou, A. Brandhuber, P. Heslop, V. V. Khoze, B. Spence and G. Travaglini, JHEP **0905**, 115 (2009) [arXiv:0902.2245 [hep-th]].
- [15] L. F. Alday, D. Gaiotto and J. Maldacena, arXiv:0911.4708 [hep-th].
- [16] L. F. Alday, J. Maldacena, A. Sever and P. Vieira, arXiv:1002.2459 [hep-th].
- [17] V. M. Braun, G. P. Korchemsky and D. Mueller, Prog. Part. Nucl. Phys. **51**, 311 (2003) [arXiv:hep-ph/0306057].
- [18] L. F. Alday and J. M. Maldacena, JHEP **0711**, 019 (2007) [arXiv:0708.0672 [hep-th]].
- [19] A. Brandhuber, P. Heslop and G. Travaglini, Nucl. Phys. B **794**, 231 (2008) [arXiv:0707.1153 [hep-th]].
- [20] V. Del Duca, C. Duhr and V. A. Smirnov, JHEP **1005**, 084 (2010) [arXiv:1003.1702 [hep-th]].
- [21] J. H. Zhang, arXiv:1004.1606 [hep-th].
- [22] K. Zarembo, JHEP **0904**, 135 (2009) [arXiv:0903.1747 [hep-th]].



- [23] A. V. Belitsky, A. S. Gorsky and G. P. Korchemsky, Nucl. Phys. B **748**, 24 (2006) [arXiv:hep-th/0601112].
- [24] N. Beisert and M. Staudacher, Nucl. Phys. B **670** (2003) 439 [arXiv:hep-th/0307042].  
• N. Beisert, Phys. Rept. **405**, 1 (2005) [arXiv:hep-th/0407277].
- [25] L. F. Alday and J. Maldacena, JHEP **0911**, 082 (2009) [arXiv:0904.0663 [hep-th]].
- [26] A. Hodges, arXiv:0905.1473 [hep-th].
- [27] M. Kruczenski, JHEP **0212**, 024 (2002) [arXiv:hep-th/0210115].
- [28] G. P. Korchemsky and G. Marchesini, Nucl. Phys. B **406**, 225 (1993) [arXiv:hep-ph/9210281].
- [29] D. E. Berenstein, J. M. Maldacena and H. S. Nastase, JHEP **0204**, 013 (2002) [arXiv:hep-th/0202021].
- [30] S. Frolov and A. A. Tseytlin, JHEP **0206**, 007 (2002) [arXiv:hep-th/0204226].
- [31] S. Alexandrov and P. Roche, arXiv:1003.3964 [hep-th].
- [32] N. A. Nekrasov and S. L. Shatashvili, arXiv:0908.4052 [hep-th].
- [33] D. Gaiotto, G. W. Moore and A. Neitzke, arXiv:0807.4723 [hep-th].
- [34] D. Gaiotto, G. W. Moore and A. Neitzke, arXiv:0907.3987 [hep-th].